COMPARISON OF OBJECT AND PIXEL-BASED CLASSIFICATIONS FOR LAND-USE AND LAND COVER MAPPING IN THE MOUNTAINOUS MOKHOTLONG DISTRICT OF LESOTHO USING HIGH SPATIAL RESOLUTION IMAGERY

By

Mpho Gegana (1257041)

Research Report submitted in partial fulfilment for the degree of Master of Science (Geographical Information Systems and Remote Sensing)
School of Geography, Archaeology and Environmental Studies, University of the Witwatersrand, Johannesburg

Supervisor: Dr Elhadi Adam
Co-supervisor: Prof Jasper Knight
Dr Zama Eric Mashimbye - Agricultural Research Council

August 2016

Declaration

I **Mpho Gegana (1257041)** is a student registered for **Master of Science Geographical Information Systems & Remote Sensing** in the year **2015/16**. I hereby declare the following:

- I am aware that plagiarism (the use of someone else's work without their permission and/or without acknowledging the original source) is wrong.
- I confirm that ALL the work submitted for assessment for the above course is my own unaided work except where I have explicitly indicated otherwise.
- I have followed the required conventions in referencing the thoughts and ideas of others.
- I understand that the University of the Witwatersrand may take disciplinary action against me if there is a belief that this is not my own unaided work or that I have failed to acknowledge the source of the ideas or words in my writing.

Signature:_____ Date 23rd August 2016

Abstract

The thematic classification of land use and land cover (LULC) from remotely sensed imagery data is one of the most common research branches of applied remote sensing sciences. The performances of the pixel-based image analysis (PBIA) and object-based image analysis (OBIA) Support Vector Machine (SVM) learning algorithms were subjected to comparative assessment using WorldView-2 and SPOT-6 multispectral images of the Mokhotlong District in Lesotho covering approximately an area of 100 km2. For this purpose, four LULC classification models were developed using the combination of SVM –based image analysis approach (i.e. OBIA and/or PBIA) on high resolution images (WorldView-2 and/or SPOT-6) and the results were subjected to comparisons with one another. Of the four LULC models, the OBIA and WorldView-2 model (overall accuracy 93.2%) was found to be more appropriate and reliable for remote sensing application purposes in this environment.

The OBIA-WorldView-2 LULC model was subjected to spatial overlay analysis with DEM derived topographic variables in order to evaluate the relationship between the spatial distribution of LULC types and topography, particularly for topographically-controlled patterns. It was discovered that although that there are traces of the relationship between the LULC types distributions and topography, it was significantly convoluted due to both natural and anthropogenic forces such that the topographic-induced patterns for most of the LULC types had been substantial disrupted.

Dedications

This report is dedicated to the memories of late Maitelwa Julius Gegana and Mbengeni “Mateki” Nengwenani

Acknowledgements

Firstly, I would like to convey my genuine gratefulness to my supervisors: Dr E Adam, Prof J Knight and Dr E Mashimbye for their unceasing sustenance, tolerance, enthusiasm and immense understanding of the subject during the course of this journey. Their guidance assisted me throughout the processes of research and also the writing-up. I could have never imagined having better team of supervisors and mentors for my MSc studies.

Besides my supervisors, I would like to acknowledge the National Research Foundation for the financial support. I would also like to thank the SANSA's Earth Observation Directorate for the provision of the SPOT-6 imagery products and an SRTM DEM.

Table of Contents

List of Figures

List of Tables

Abbreviations

asl	-	above sea level
ASTER	-	Advanced Spaceborne Thermal Emission and Reflection Radiometer
ATCOR	-	Atmospheric and Topographic Correction
CBERS	-	China–Brazil Earth Resources Satellite
DEM	-	Digital Elevation Models
DRS	-	Direct Receiving Station Supply, Reception and Distribution
DT	-	Decision Trees
ETM+	-	Enhanced Thematic Mapper
HRG	-	High Resolution Geometry
HRV	-	High Resolution Visible
K-NN	-	K-Nearest Neighbour
LULC	-	Land Use and Land Cover
MASTER-		MODIS/Advanced Spaceborne Thermal Emission and Reflection Radiome
MDC	-	Minimum Distance Classifier
MIR	-	Mid Infrared
MLC	-	Maximum Likelihood Classifiers
MODIS	-	Moderate Resolution Imaging Spectrometer
MRS	-	Multi-Resolution Segmentation
MSS	-	Multispectral Scanner System
NDVI	-	Normalised Difference Vegetation Index
NIR	-	Near infrared
NN	-	Neural Networks
OBIA	-	Object Based Image Analysis
PBCT	-	Probability-Bagging Classification Trees
PBIA	-	Pixel Based Image Analysis
PC	-	Parallelepiped Classifiers
PLDA	-	Penalized Linear Discriminant Analysis
PLDA	-	Poisson Linear Discriminant Analysis
QDA	-	Quadratic Discriminant Analysis
RBF	-	Radial Basin Function
RF	-	Random Forest
RGB	-	Red, Green and Blue
SANSA	-	South African National Space Agency
SDS	-	Spectral Differencing Segmentation
SPOT	-	Satellite Pour l'Observation de la Terre
SRTM	-	Shuttle Radar Topography Mission
SVM	-	Support Vector Machines

1. INTRODUCTION

1.1. Background

Land use and land cover (LULC) information is desired by land managers, government agencies, municipalities, environmentalists and other professional practitioners to facilitate decision-making and also to equip the understanding of the interactions between humans and their surrounding environment (Prakasam, 2010; Yadav *et al.*, 2010). LULC information is presently in great demand particularly due to the pressures of global population growth as it is necessary for the selection, forecasting and implementation of intervention efforts to meet the increasing demands of human needs and welfare (Yadav *et al.*, 2012). Remote sensing and Geographical Information Systems (GIS) technologies provide operative and effective methods to collect such required information and create spatial representations in form of maps which are then used by those who require them (Chena *et al*., 2009).

Remotely sensed imagery data acquired from satellite- and air-borne sensors constitute a strong foundation for LULC mapping (Aguirre-Gutiérrez *et al.*, 2012). The analysis of remotely sensed data incorporates the identification and/or quantification of target features from an imagery scene with the goal of extracting useful information. These interpretations of images may be done manually or digitally. Digital approaches are preferred over the manual approaches as they are considered to be more objective, time efficient, they utilize information from many bands that may not be observed by a naked eye, and can be easily implemented even in a large area with finer resolutions and multispectral data (Mararakanye and Le Roux, 2011; Rozenstein and Karnieli, 2011; Mararakanye and Nethengwe, 2012).

Digital image classification may be performed through either pixel-based (PBIA) or object-based (OBIA) image analysis. PBIA uses individual pixels as basic processing units while OBIA uses multi-pixel image objects made from those pixels sharing some degree of spatial and spectral characteristics (Tehrany *et al.,* 2014). Regardless of which of the two analysis approaches is applied, the information contained within and between the basic processing units, i.e. pixels or image objects are subjected to a variety of classification algorithms (Duro *et al.,* 2012).

Comparative studies on the performances of the PBIA and OBIA approaches LULC types extraction have been conducted for various types of landscapes. Such landscapes includes heterogeneous coastal landscapes using RapidEye imagery by Adam *et al.* (2014),

agricultural lands using SPOT-5 by Duro *et al.* (2012), coastal urban areas using SPOT-5 by Tehrany *et al.* (2014), and urban areas with Landsat ETM+ by Adepoju *et al.* (2015). A more comprehensive summary of the comparisons and the achieved performances is provided in the literature review section of this study. Although comparative studies of the two approaches have been done, it is evident that there have been limited studies done on mountainous landscapes.

This study sought to conduct comparative evaluations on the performances of the supervised PBIA and OBIA classifications for LULC in a mountainous landscape. Previous comparative studies utilized multispectral datasets such as LANDSAT, ASTER and MODIS which provide both extensive coverage and relatively cheaper imagery datasets. However, the map products from these images, particularly at fine scale in heterogeneous areas, are characterised with salt-and-peppers effects due to the deficiency in spectral and spatial resolutions compared to the target LULC classes (Blaschke *et al.,* 2006). Therefore, LULC maps produced from data from the above sensors are often regarded as of insufficient quality for operational application purposes, due to disparities between the reference dataset and predicted classes from the imagery used (Foody, 2002).

Hyperspectral sensors have recently emerged as the alternative to multispectral sensors and have been utilised in the detection of land surface objects in plentiful and finer continuous spectral bands, which therefore allow for better differentiation amongst comparable target LULC classes in contrast to the more commonly known and used multispectral images (Petropoulos *et al.,* 2012a). Findings from such studies show the potential for accurate LULC mapping and extraction using hyperspectral data from remote sensing (Pal, 2006; Pignatti *et al.,* 2009; Petropoulos *et al.,* 2012b). However, the use of hyperspectral datasets for any remote sensing applications comes with challenges, particularly prices, accessibility, processing requirements and dimensionalities (Mutanga *et al.,* 2012).

This study made use of SPOT-6 and WorldView-2 multispectral images for the extraction the LULC types. The two imagery packages used in this study are of "moderate resolutions" and are understood as a sense of balance between the advantages of multispectral and hyperspectral data (Mutanga *et al.,* 2012). SPOT-6 data are freely available to government and academic institutions in South Africa and other African countries through the South African National Space Agency (SANSA) (van Zwieten, 2014), on the other hand the WorldView-2 is available at a price. Therefore this study also sought to understand if it is

advisable for LULC mappers to use the freely available SPOT data or to go on procuring higher resolution data such as WorldView-2, when seeking to map mountainous landscapes.

1.2. Problem Statement

Landscapes are heterogeneous and complex spatial units which have a potential to supersede the capabilities of remote sensing techniques of capturing these complexities (Blaschke *et al.*, 2006). LULC types as components of landscapes present some difficulties when being distinguished from a remote sensing perspective, particularly on an uneven terrain. The complexities characterising LULC dynamics on uneven terrains (mountainous landscapes) are due to the variations in terms of the rainfall and insolation as a result of the variations of landscape altitudes, slope and aspect leading to heterogeneity of vegetation and other components of ecosystems (Salman *et al.,* 2002; Wondie *et al.,* 2012).

Numerous comparative studies of PBIA and OBIA have been conducted for various types of landscape and their complexities including urban, coastal and other areas. Generally, research has shown that the OBIA approach outclasses the PBIA in terms of their overall classification accuracies when using different imageries on different settings (Adepoju et al., 2015). However, the outcomes may have been due to the fact that most of these comparison studies often relied on simple classification algorithms for an OBIA approach, and Gaussian-based parametric algorithms for a PBIA approach (Duro *et al.,* 2012). The use of parametric classifiers was discouraged for use in datasets that do not meet the assumptions of normality (Duro *et al.,* 2012).

In fact, the use of parametric classifiers is discouraged in the classification of complex spectral heterogeneous landscapes (Pradhan *et al.,* 2014; Tehrany *et al.,* 2014). The use of non-parametric classifiers such as Support Vector Machines (SVM), Neural Networks (NN) and Random Forest (RF) is encouraged due to the fact that they do not employ any assumption on the statistical relationship between the provided training dataset and also able to accommodate the addition of ancillary data that may be handful in the improvement of the overall accuracies (Pradhan *et al.,* 2014; Tehrany *et al.,* 2014).

This study intends to fill the gaps that may have been left by previous comparative studies through the examination of performances of the relatively contemporary, vigorous and non-parametric supervised machine learning algorithms of SVM. This study was envisioned as a contribution for improving the understanding of mapping LULC on complex mountainous terrains of Mokhotlong District of Lesotho by attempting to identify the best combination of sensors' images and landscape characteristics.

1.3. Research Objectives

1.3.1. Research Aim

The aim of this study is to compare the performance of pixel-based and object-based image analysis approaches for LULC classification on a mountainous landscape using different high resolution images.

1.3.2. Research Objectives

The primary objectives of this study are to:

i. Compare SPOT-6 and WorldView-2 high resolution imagery for their suitability for mapping LULC in a mountainous landscape.
ii. Evaluate the performance of PBIA and OBIA SVMs in mapping LULC on mountainous landscape from SPOT-6 and WorldView-2.
iii. Assess the relationship between the extent and distribution of LULC classes with topographical variables (i.e. slope, altitude and aspect).

1.3.3. Research Questions

This study was guided by the following research questions:

i. Does the difference in spatial and spectral resolutions between SPOT-6 and WorldView-2 high resolution imageries translate to significant difference in the performances for LULC mapping of mountainous landscape?
ii. Which between the OBIA and PBIA approaches has a better accuracy in mapping mountainous landscape than the other?
iii. What is the relationship between the distribution of LULC and topography in the study area?

2. LITERATURE REVIEW

2.1. The remote sensing of LULC

Land use refers to the activity which human perform on a particular piece of land, whereas land cover refers to the definite material covering the surface such as vegetation, structural and others that may be as a result of dedicated use for that piece of land (Sohl *et al.,* 2010). Land cover is made of patterns that occur due to a variety of natural and anthropogenic processes, whereas land use is largely due to by economics, social, political and historical factors (Rozenstein and Karnieli, 2011; Şatır and Berberoğlu, 2012). The increasing obtainability of images due to the prompt improvements of remote sensing technologies expanded the pool from which imagery products may be chosen (Xie *et al.,* 2008).

The use of remotely sensed images for the extraction of LULC targets has an extensive history, even prior the establishment of the initial Landsat platform in the early 1970s (Sohl *et al.,* 2010). Remote sensing sensors which serve as sources of the imagery datasets are known for their variances in spectral, spatial, radiometric and temporal qualities associated with those resolutions. Sohl *et al.* (2010) cautioned the use of imagery data alone for the mapping of land use, in contrast to land cover, which may be directly detected and examined from the imagery. In fact land use should be inferred through a combination of image interpretation, some field familiarity with the study area, and other supplementary information that may provide an enhanced correlation between land cover and land use (Sohl *et al.,* 2010).

Nanyam *et al.* (2011) acknowledged the challenge hampering automated successful LULC mapping as dependent on elements such as the complexity of site. Remote sensing and GIS offer an opportunity for the analysis of the relationship of LULC distribution with topography with respect to elevation, slope and aspect. Despite various ongoing efforts, gaps still exist on the understanding of the spatial distribution of land cover with respect to these topographic variables (Wondie *et al.,* 2012). The characteristic spatiotemporal complexity of LULC classes in mountainous landscapes may hinder the accuracy scores of remote sensing data (Okubo *et al.,* 2010; Li and Shao, 2014). The improvements and increase of sensors that provide imagery with higher spatial and spectral resolution assists in the production of more detailed mapping of LULC (Ramaswamy and Ranganathan, 2014). The heterogeneity of mountainous landscapes may lead to spectral distinction within the identical and spectral confusion amongst different categories at finer spatial resolution, hence yielding poorer classification performances (Ramaswamy and Ranganathan, 2014). The overall accuracy

levels of classifying LULC of complex, spectrally heterogeneous landscapes from high-spatial resolution imagery can be enhanced by factoring in ancillary data such as a digital elevation model (DEM) and its derivatives, i.e. slope and aspect (Li and Shao, 2014).

2.2. Mountainous landscapes: characteristics and LULC mapping

The natural environments of mountainous landscapes can best be characterized by their diversity (Nagakura, 2010). The characteristic diversity of a mountainous landscape includes the wide range of altitudes, slopes and aspects which then influence the variation in temperatures, varying rates of erosion which leads to a variation of landforms (Bennie *et al.*, 2006; Nagakura, 2010, Tovar *et al.,* 2013). The characteristic steep slopes, cold temperatures and snowfalls offer environmental constraints to life as these conditions make it difficult to sustain livelihoods in such regions (Nagakura, 2010). Mountain regions are generally characterised with rich biodiversity and are currently under threats of LULC changes due to climate change. Hence efficient observations are required to capture such changes (Tovar *et al.,* 2013).

Remote sensing is of great use for the mapping of LULC in mountainous areas as accessibility is limited and land degradation is a great concern (Shrestha and Zinck, 2001).Various algorithms for mapping LULC are available. Nonetheless they face challenges when employed in areas with strong topographic variations such as mountainous areas (Shrestha and Zinck, 2001). In these areas, results obtained by running classifications are deficient for mapping LULC with the main reasons being altitudinal and illumination variations, and influence of topographic shadow (Shrestha and Zinck, 2001). Variations in topography have an effect on microclimates, which may translate into variations in LULC patterns which then pose a challenge for spectral classifications.

2.3. Comparisons of feature extraction or classification applications from images with various resolutions

Novack *et al.* (2011) conducted a comparative assessment of pan-sharpened WorldView-2 and QuickBird-2-simulated images with regards to their prospects of being utilised for object-based urban LULC mapping. The study found that the presence of four extra spectral bands and the spatial resolution of the WorldView-2 offers an enhanced opportunity for the extraction of LULC types in different types of landscapes. The performances of the WorldView-2 and Quickbird imageries were also assessed by Belgiu and Dragut (2014) for

supervised and unsupervised multi-resolution segmentation (MRS) approaches for extracting buildings. Belgiu and Dragut (2014) found that the two approaches produced extraordinarily comparable classification results, with overall accuracy scores ranging between 82 and 86%.

Lu *et al.* (2005) compared the capabilities of Landsat TM, ASTER, and SPOT imagery data in LULC classification in the Amazon basin using pixel-based MLC. The study by Lu *et al.* (2005) found that different sensor data have their own merits for LULC classification and none of the images used produced best classification results for all the classes. The main conclusion from the above study is that the increase spatial resolution is useful for the enhancement of the overall accuracy scoring. Gao and Mas (2013) conducted a study which intended to determine the impact at which the spatial resolution influence the overall performances of object-based classifications. Gao and Mas (2013) used two images with four varying spatial resolutions and found that the OBIA performed better than the PBIA; with an increased spatial resolution, the range of the difference on the performance scoring was reduced. Gao and Mas (2003) concluded that the OBIA had an advantage over the PBIA, and in accuracy rating, the advantage was better represented by higher spatial resolution satellite images.

Capolsini *et al.* (2014) conducted a comparative study of Landsat ETM+, SPOT HRV, IKONOS, ASTER, and MASTER data to map the habitats of coral reefs in the South Pacific Islands using a supervised MLC. The findings of Capolsini *et al.* (2014) in terms of accuracy revealed that the Landsat-7 ETM+ performed relatively well compared with images from sensors with better spatial and spectral resolutions (IKONOS and MASTER) in mapping low and moderate habitats, even though it is well known that the two sensor have significantly better spatial and spectral resolutions compared to Landsat. However, during the mapping of highly convoluted habitats, IKONOS imagery performed best, suggesting the significance of the high spatial resolutions; and for low and moderate complex mapping, MASTER performed best, signifying the importance of spectral resolutions.

Ambinakudige *et al.* (2009) paralleled the performances of LANDSAT-7 and the Chinese Brazilian Earth Resource Satellite (CBERS) images for LULC mapping using an unsupervised classification algorithm. The two images are very similar in terms of quality and spectral band characteristics, but are significantly different in terms of spatial resolutions. The Landsat and CBERS have the spatial resolutions of 30 m and 20 m, respectively. Ambinakudinge *et al.* (2009) found that the two images produced similar trends in terms of their correlations with NDVI due to their spectral and image qualities, however the CBERS

outperformed the Landsat in terms of LULC mapping due to its better spatial resolution and was recommended for future use over LANDSAT.

2.4. Algorithm comparisons using PBIA or OBIA classifications

As aforementioned, image classification can be conducted through the "traditional" PBIA and the "modern" OBIA approaches (Tehrany *et al.,* 2014). The PBIA approach is the more prevalent of the two and involves the use of spectral characteristics related to each individual pixel. It is used to distinguish between classes, as each feature type is made of unique combination of digital numbers or spectral signatures (Pradhan and Suleiman, 2009). The main limitation of the PBIA approach is that during the classification processes only the spectral aspect of a feature is used, discounting the spatial, textural and topological relationships of pixels (Matinfar *et al.,* 2007; Bhaskaran *et al.,* 2010). The other shortcoming of the PBIA, particularly when mapping complex spectrally heterogeneous settings to produce maps with unclassified pixels (Blaschke *et al.,* 2006).

These shortcomings of the PBIA led to the emergence of the OBIA approach as an alternative to pixel-based image processing (Myburgh and Van Niekerk, 2013). The OBIA approach delineates readily functional image objects from imagery while concurrently exploiting image processing and GIS functionalities in order to utilize spectral and spatial information in an integrative way (Blaschke, 2010). The OBIA approach offers satisfactory and automatic techniques for the analysis of high resolution imagery by describing the imaged reality using spectral, textural, spatial and topological characteristics (Lang, 2008). The OBIA offers a procedural framework for the explanation of complex categories arranged by their relative similarities in spectral, spatial and structural properties (Lang, 2008).

2.5. Algorithm comparisons using PBIA or OBIA classifications

The PBIA approach was applied in a LULC mapping study by Huang *et al.* (2002) using Landsat TM data with thematic mapping accuracies produced using SVM, Decision Trees (DT), NN and MLC classifications. The SVM-based classifications outperformed the rest of the used classifiers. In Pal (2005), the accuracies of SVMs and RF supervised classification algorithms were conducted using a Landsat ETM+ data for an urban land cover mapping and the performances were not statistically different. The selected RF algorithm was compared to the DTs using a PBIA and the RFs gave the best results for the classification of LULC using the Landsat Multispectral Scanner System (MSS) (Gislason *et al.,* 2007).

Carreiras *et al. (*2006) studied the performances of pixel-based classifiers such as DT, Probability-Bagging Classification Trees (PBCT) and K-NN on SPOT4 data. The PBCT produced best overall classification accuracies (Carreiras *et al.,* 2006). Brenning (2009) conducted a comprehensive comparison study of at least eleven classification algorithms using a PBIA on Landsat ETM+ imagery for the detection of rock glaciers, and the Poisson Linear Discriminant Analysis (PLDA) produced considerably improved results as compared to all other classifiers. Otukei and Blashcke (2010) conducted a land cover change assessment in which the performances of DT's, SVMs and MLCs algorithms in PBIA approach using Landsat TM and ETM+ data, and found that the DT's performed better than the other two classifiers.

An OBIA approach was conducted by Laliberte *et al.* (2006) using Quickbird imagery comparing the K-NN and DT. The study found that DTs were better performers in terms of their overall classification accuracies. Duro *et al.* (2012) conducted a comparison of PBIA and OBIA approach using RFs, SVMs and DTs for the classification of farming landscapes using SPOT-5 imagery. Duro et al (2012) used an OBIA approach and found that there was statistically significant difference in the performances of DT when compared with both RF and SVM algorithms, while when PBIA was employed there was no significance in the differences at $\alpha>0.05$ between overall performances of the classifiers. Adam *et al.* (2014) conducted a LULC classification study of a coastal landscape through the assessment of the performance of RF and SVM algorithms. The authors found that the performances of the two classifiers were not significantly different as had been found through the performance of a McNemar's test.

2.6. Algorithm comparisons between PBIA and OBIA classifications

Comparative studies between the performances between the PBIA and OBIA have also been piloted. For example, Tehrany *et al.* (2014) compared the two approaches for mapping LULC using SPOT 5 imagery and found that the OBIA K-NN performed better than the PBIA DT classifiers and OBIA SVMs. A similar study was conducted by Yan (2006) who compared PBIA using MLC and OBIA on a ASTER imagery, and their study found that the accuracy of the K-NN classification significantly outdid the MLC (83.25% and 46.48%, respectively). Myint *et al.* (2011) used similar algorithms as Yan *et al.* (2006) but for the classification of urban LULC on Quickbird imagery, and found that the performances were the same as the OBIA approach significantly outperformed the PBIA approach.

Castillejo-González *et al.* (2009) compared the performances of PBIA and OBIA, seeking to find the best imagery and classification algorithms combination for LULC classification. Their study found that there was a small difference between the two approaches using a non-pansharpened imagery; however, the difference between these approaches amplified significantly when using a pan-sharpened product. K-NN and MLC were compared for both classification approaches on multispectral IKONOS imagery by Platt and Rapoza (2008) and the findings were that the K-NN performed better than MLC. Robertson and King (2011) conducted the study for classified LULC for a broad agricultural landscape over two time periods. The LULC maps produced using pixel based MLC and object-based K-NN algorithms were not statistically significantly different in terms of their overall accuracies.

2.7. The role of topography in the distribution of LULC

Vegetation communities are fixed and require specific environmental conditions; thus, the spatial structure of vegetation communities exists through specific habitat preferences or niches (Lowe *et al.,* 2012). The combination of climate and other environmental factors, such as topography, are widely used to explain the spatial distribution of LULC types (Guisan and Zimmerman, 2000; Zhao *et al.,* 2010; Lowe *et al.,* 2012).Topography has a significant effect on the physical and environmental settings that affect patterns of LULC particularly vegetation (Franklin *et al.,* 2000; Matsuura and Suzuki, 2013; Zhang *et al.,* 2013). The understanding and explaining of the spatial distribution of LULC dynamics across landscapes is of paramount importance in natural resource management sciences (Guisan and Zimmerman, 2000; Coblentz and Keating, 2008). Variation in relief and topography (i.e. elevation, slope, and aspect) are considered to be main factors prompting LULC due to their effect on site-specific microclimatic dynamics (Coblentz and Keating, 2008; Zhao *et al.,* 2010, Wondie *et al.,* 2012). Elevation or altitude refers to the positional height of a feature in relation to sea level; aspect is the compass direction that a slope faces; hence the slope angle is the measure of change in elevation with respect to distance (Bennie *et al.,* 2006).

The altitudinal position of an object affects temperature with locations higher relative to sea level being cooler than those on lower slopes (Bennie *et al.,* 2006). As a result of the above described variations, the lower slopes of the landscapes tend to be characterised by primary productivity compared to those at higher elevations. Aspect regulates the quality and quantity of direct solar radiation received by a slope, which in turn influences temperature and shading from the sun (McCune and Kean, 2002; Bennie *et al.,* 2008). Surfaces receiving

less insolation generally experience cooler and, therefore, moister microclimates, whereas surfaces receiving more incoming solar radiation generally experience warmer and congruently dryer conditions (McCune and Kean, 2002). In the southern hemisphere, slopes that are facing northwards are commonly exposed to direct sunlight than other slopes which are generally shaded and cooler, as are south-facing slopes in the northern hemisphere.

Moreover, the slope angle of a feature impacts wind and water characteristics on a site, hence the steeper the slope the higher the velocity of wind and upward movement of the wind. The steepness of the slope also influences the speed of run-off, meaning that there is less period for infiltration into the soil and so be made accessible to plants, but correspondingly more likely to erode the soil on the slope, mostly when heavy rainfall occurs (Bennie *et al.,* 2006; 2008). Furthermore, slope may act as an important input for microclimatic conditions affecting the growth and distribution of vegetation (Bennie *et al.,* 2008). Steeper slopes generally receive greater concentrations of incoming solar radiation and therefore experience warmer, dryer climates than slopes with decreased steepness (Bennie *et al.,* 2008). Slope also affects soil moisture through downslope drainage, with greater rates of drainage occurring on steeper slopes (Maestre *et al.,* 2003).

These relationships between topographic variables and the distribution of LULC types are subject to complexities particularly on landscapes that have been altered (Hoersch *et al.,* 2002). Landscapes may be altered due to natural disturbances (e.g., fires, drought), anthropogenic activities (e.g., agriculture, deforestation) or combinations of both. These alterations tend to lead to the disruption of topographic-induced patterns in terms of the distribution of LULC types across a landscape (Hoersch *et al.,* 2002). Moreover, random distributions of LULC types like vegetation are possible, but there is evidence which suggests that in topographic variable landscapes such as mountains, particularly in the mid-to-high latitudes, the distribution of vegetation can be correlated to topography (Hoersch *et al.,* 2002; Coblentz and Riitters, 2004; Pérez *et al.,* 2008; Lowe *et al.,* 2012).

3. MATERIALS AND METHODS

3.1. The study area

The area of study is situated within the Mokhotlong District; north-eastern parts of the mountainous kingdom of Lesotho (Figure 3-1). It covers an elevation range of 2000 – 3000 m, with an average of about 2300 m and encompasses just over 100 km^2. Lesotho lies in the middle of the Drakensberg Mountains in southern Africa and is characterised by a tropical mountain climate with a seasonal rainfall from October to March, and a prominent dry season of limited rainfall around June and July (Sene *et al.*, 1998; Nagakura, 2010). The north-eastern parts of Lesotho where the study area is located receive more precipitation in summer than any other region in the country (Kobisi, 2005). Generally, as per the Köppen Climate Classification system, Lesotho is characterised by a maritime temperate climate (Nagakura, 2010).

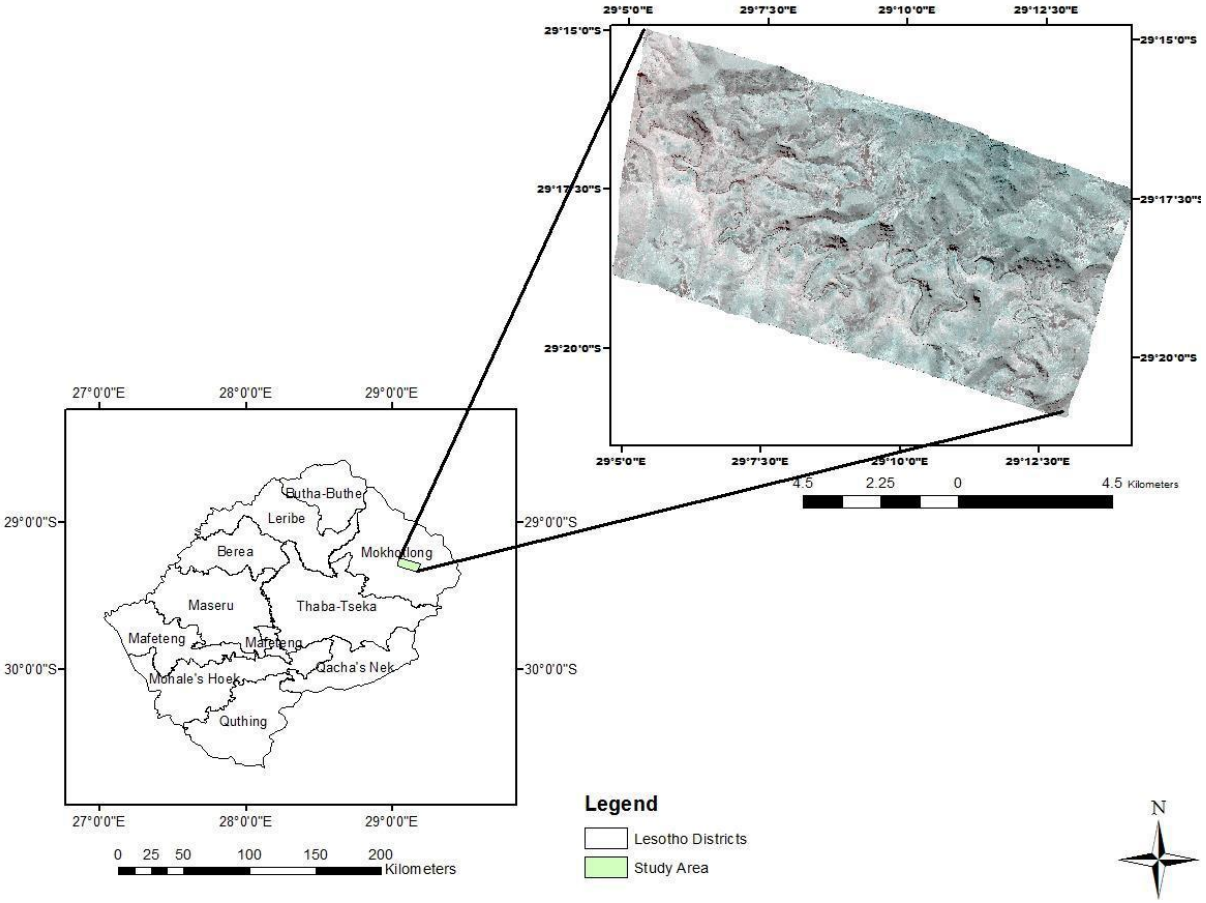

Figure 3-1: The study area

The study area is situated within the undulating mountain plateau of eastern Lesotho and is restricted by the rocky obstruction of the High Drakensberg Mountains (Nagakura, 2010). The study area, Mokhotlong District is situated in the mountainous (highlands) agro-ecological zone (Moeletsi and Walker, 2013). The climate in the Mokhotlong District is temperate; is slightly suitable for crop agri-business due to unpredictable and spatially variable precipitation that ranges from 500 mm/year to ~1200 mm/year in a few areas around Mokhotlong (Moeletsi and Walker, 2013). Monthly mean minimum temperatures in winter range between −6.3°C in the highlands to 5.1°C in the lowlands; freezing temperatures are common in the winter months (May to July) but may also occur during summer (Moeletsi and Walker, 2013). Monthly mean maximum temperatures occur between November and February (Moeletsi and Walker, 2013). The vegetation in the Mokhotlong District ranges sharply from the trees and scrublands bush of the slopes to the characteristic mountain grassland on plateau tops with high solar radiation, sturdy winds, basaltic soils, and low temperatures (Kobisi, 2005). These factors bound the growth of plants in terms of height; such that vegetation occurring in these areas tends to be very short excluding the shielded valleys where perennial green trees and shrubs grow well (Kobisi, 2005).

3.2. Materials

The high spatial resolution imagery that were used in this study are SPOT-6 and WorldView-2. An orthorectified WorldView-2 imagery captured on the 11th November 2014 was sourced from Digital Globe through Southern Mapping. The WorldView-2 imagery package included panchromatic and multispectral images; on the other hand a level 1A SPOT-6 imagery package of the same date was sourced from the SANSA's Earth Observation Directorate (refer to Table 3-1 below for their specifications). A DEM from the Shuttle Radar Topography Mission (SRTM) programme with a grid spacing of 30 m was used for the geo-referencing the SPOT-6 imagery and also for the derivation of the three topographic variables that were then used in the study of the relationship between LULC types and topography. The SRTM DEM mosaic for the entire SADC region was obtained from the 2015's SANSA Earth Observation FUNDISA disc.

3.3. LULC mapping

The three standard steps of image classification for LULC mapping followed in this study: pre-processing, classifications and accuracy assessment are discussed below:

3.3.1. Image pre-processing

Image pre-processing is essential prior to the extraction of information from the imagery as it ensures that the image is of similar radiant energy and spatial characteristics as when the image was captured. Pre-processing is comprised of mandatory steps: geometric correction or image registration, atmospheric correction and radiometric calibration, and some additional processes such as topographic correction and noise reduction that are also applied when necessary (Şatır and Berberoğlu, 2012; Iqbal and Khan, 2014). Topographic corrections are only necessary on imagery of irregular topography such mountain ranges and noise removal is performed when pixel values do not reflect the true intensities of the real scene.

Table 3-1: SPOT-6 and Worldview-2 satellites and HRG instruments details

Satellite/Sensor properties	**SPOT-6**	**WorldView-2**
Orbit	Sun synchronous	Sun synchronous
Equator crossing time	10:00 am local time	10:30 am local time
Spectral bands and spatial resolutions (HRG)	4 multispectral bands at 6.0 m resolution (blue, green, red, near infrared (NIR))	Single panchromatic band at 50 cm resolution 8 multispectral bands at 2.0 m spatial resolution (Coastal, Red, Blue, Red Edge, Green, NIR1, Yellow, NIR 2)
Spectral range (HRG)	Panchromatic(450 – 745 nm) **Multispectral** Blue (455 – 525 nm) Green (530 – 590 nm) Red (625 – 695 nm) NIR (760 – 890 nm)	Panchromatic (450 – 800 nm) **Multispectral** Coastal (400-450 nm), Red (630-690 nm),Blue (450-510 nm), Red Edge (705-745 nm), Green (510-580 nm), NIR1 (770- 895 nm),Yellow (585-625 nm)& NIR2 (860-1040 nm)
Data quantisation	12-bits per pixel	11-bits per pixel
Imaging swath	60 km at nadir	16.4 km at nadir

The pre-processing stage was only necessary on the SPOT imagery and was conducted on an ERDAS 2014 Imagine® environment. The SPOT imagery bands were subjected to atmospheric and topographic corrections, and orthorectification. The atmospheric and topographic corrections were completed with the Atmospheric and a Topographic Correction (ATCOR) 3 module as it was designed for applications on the uneven and mountainous terrains. Orthorectication was applied using a nearest neighbour algorithm using the parameters shown on Table 3-2.

Table 3-2: Orthorectification projection parameters for the SPOT 6 Imagery package

Projection type	Universal Transverse Mercator
Spheroid	WGS 1984
Datum	WGS 1984
Scale factor at central meridian	0.9996
Longitude of central meridian	27 E
Latitude of origin projection	0
False easting	500000 meters
False northing	-10000000 meters

3.3.2. LULC class definition and sampling

The initial classification was comprised of 18 spectral classes generated from the pan sharpened product of 0.5 meters panchromatic Worldview-2 and the 8 multispectral bands of WorldView-2 using the ISO Cluster Unsupervised Classification technique on ArcMap 10.3®. The 18 spectral classes achieved from the ISO clustering technique were regrouped into 9 broad LULC classes listed and described on Table 3-3, which were then used in this study.

Table 3-3: LULC classes and descriptions

CLASS	**DESCRIPTION**
Water bodies	All areas of open water
Bare soil	Non-vegetated barren areas dominated by loose soil and sand, does not include those used for agricultural purposes
Cultivated	Large-scale area with soil tilled for agricultural purposes.
Green vegetation	Green, tall trees and bush dominated areas, typically with higher canopy heights and more compact canopy densities
Shadows	Surfaces at which the sunlight was obstructed by the opaque surrounding such that the sensor couldn't capture the true LULC type
Burnt areas	Surface characterised with dark/black ashes showing signs of having had experienced fires recently
Scrubland	Grass and shrubs which did not particularly look green in colour. Most looked dry and may have survived the recent fire outbreaks
Rock outcrops	Non-vegetated areas dominated by protruding rock fragments
Built-up areas	Rooftops of man-made structures typically made from shiny corrugated iron sheets and other materials

The generalised ISO Clustering classification of the pan-sharpened WorldView-2 was then converted into polygon based maps using the class value as the basis for the conversion.

Stratified random sample pixels within each LULC types were performed. The collected samples were then used as ground reference data, as contemporary field-collected samples were not available from the selected study area. A stratified sampling frame was employed in the collection of reference samples with no consideration of how prominent they seem to have occurred judging from the unsupervised classification. Equal numbers of samples per class was collected (Duro *et al.,* 2012). A total of 774 pixels were selected (86 per LULC class). The reference data were then allocated randomly into training and validation /datasets (Table 3-4) using the 70/30 rule for each class by generating a list of 60 random unique numbers within a range of 1 to 86 on Microsoft Excel 2013®. The samples whose number corresponded with random unique numbers generated on Excel were used to train the classification algorithm and the remaining 26 were used for validations.

Table 3-4: Training and validation data set for the LULC classes

LULC Classes	Training # pixels	Validation # Pixels	TOTAL # of pixels
Water bodies	60	26	86
Bare soil	60	26	86
Cultivated	60	26	86
Green vegetation	60	26	86
Shadows	60	26	86
Burnt areas	60	26	86
Dry vegetation	60	26	86
Rock outcrops	60	26	86
Built-up areas	60	26	86
TOTAL	540	234	774

3.3.3. Support Vector Machine Classification Algorithms

For classification purposes, the pixel-based and object-based SVM algorithms were used. The SVMs are cluster of supposedly superior machine learning algorithms which are found to be uncertain with the best available in categorizing high-dimensional datasets (Huang *et al.,* 2002). The success of the classification accuracies of the SVMs depends on: how well the training was conducted, the kernel used, tune parameters chosen to fit the kernel and the method used to produce the SVM (Huang *et al.,* 2002; Otukei and Blascke, 2010). The SVM algorithms calculate the optimal separating hyper-plane between classes using the support vectors (training data) placed at the edges of class descriptors (Tzotsos, 2006).

There are four kernel types used in SVM classification, i.e. linear, polynomial, radial basis function (RBF) and sigmoid. The RBF kernel used for this study, with the rest having had been considered. The RBF kernel was a preferable choice over others because it nonlinearly maps the provided support vectors into higher dimensional spaces (Hsu *et al.*, 2010). The tuning parameters for the SVM models utilising the RBF kernel are Gamma Kernel Function (GKF) and the penalty parameter. The increasing in the GKF was kept at the default 0.125 and the penalty parameter at 100.0.

3.3.4. PBIA

The PBIA approach is essential for the recognition of spectral patterns across the study area. This approach was exclusively applied in an ENVI 5.2® environment for both images. The workflow of the applied PBIA methodology is shown in Figure 3-2.

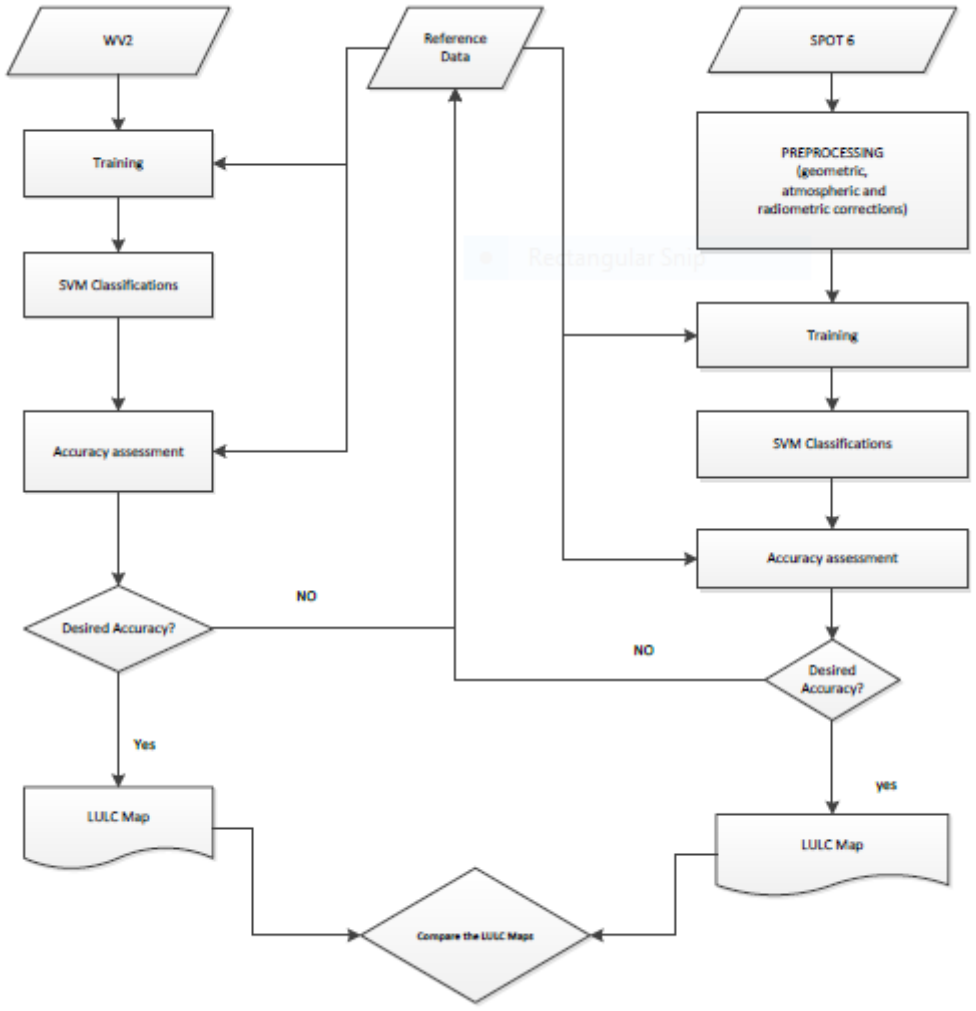

Figure 3-2: Main stages of LULC mapping through PBIA approach of both SPOT-6 and WorldView-2

3.3.5. OBIA

This OBIA approach is essential for the recognition of spatial patterns across the study area as it integrates spectral and spatial characteristics for its classifications. The OBIA classification process is generally preceded by segmentation

3.3.5.1. Segmentation

Segmentation serves an initial step of OBIA and generally involves the creation of image-objects that represent meaningful entities by assembling neighbouring pixels with similar characteristics (Cleve *et al.,* 2008). This study made use of the Multi-resolution (MRS) and spectral differencing segmentation (SDS) image segmentation algorithms found in the 64-bit version of eCognition Developer 9® environment (Trimble, 2014).

The MRS algorithm is a bottom-up approach which is based on the pairwise region merging technique which, for a given number of image objects, lessens the average heterogeneity and maximizes their respective homogeneity (Trimble, 2014). The MRS process commences with pixel-sized objects which are then iteratively established through pair-wise amalgamation of adjacent objects based on several predefined scale, colour, shape, smoothness and compactness parameters (Duro *et al.,* 2012). These parameters are the subjected to relative weighting in order to define the homogeneity measure, and a "stopping threshold" of within-object homogeneity based on underlying input layers, and thus can explain the size and shape of resultant image objects (Duro *et al.,* 2012; Trimble, 2014).

The scale parameter is considered as the most crucial of the MRS process as it controls the relative size of the image object, which directly affects the overall accuracy of classifications (Benz *et al.,* 2004; Pakale and Gupta, 2010; Myint, *et al.* 2011; Trimble, 2014). The shape and compactness factors use weights ranging between 0 and 1 to control the homogeneity of the image objects at different scales (Pakale and Gupta, 2010). The shape factor regulates spectral homogeneity versus the shape of objects, while the balance between compactness and smoothness controls the shape between smooth boundaries and compact edges (Pakale and Gupta, 2010; Myint *et al.,* 2011). The smoothness factor is directly linked to the compactness and their sum equals to one, and are only effective when the shape factor is larger than zero (Myint *et al.,* 2011; Trimble, 2014)

The SDS allows for the image objects to be merged, provided that their mean spectral intensities are less than or equal to the value given as the mean maximum spectral difference parameter (Trimble, 2014). The SDS is also a bottom-up segmentation approach, as it was designed to in order to refine the existing segmentation results by merging spectrally similar

image objects produced by previous segmentations, and cannot be used to develop image object based on the pixel level (Trimble, 2014). For the purpose of this study, the same segmentation rules and parameters were applied at 3 m scale so that small features such as the built-up structures are captured during the segmentation. All the image layers were given an equal weight of 1 except for the NIR1 weight value which was doubled on both images. The parameters used for the segmentation on both imageries are as shown in Table 3-5:

Table 3-5: Parameters for the segmentations for the imagery scenes

Level 1	MRS	Composition Of Homogeneity Criterion	Scale Parameter	3
			Color	0,7
			Shape	0,3
			Smoothness	0,9
Level 2	SDS		Compactness	0,1
			Maximum Spectral Difference	10

During training of the OBIA approach a class hierarchy is developed which involves the selection of representative of different LULC types. The description of classes is achieved through the combination of mean, standard deviations, and ratio of imagery bands (Volker, 2003). The steps followed for the OBIA approach is shown on Figure 3-3.

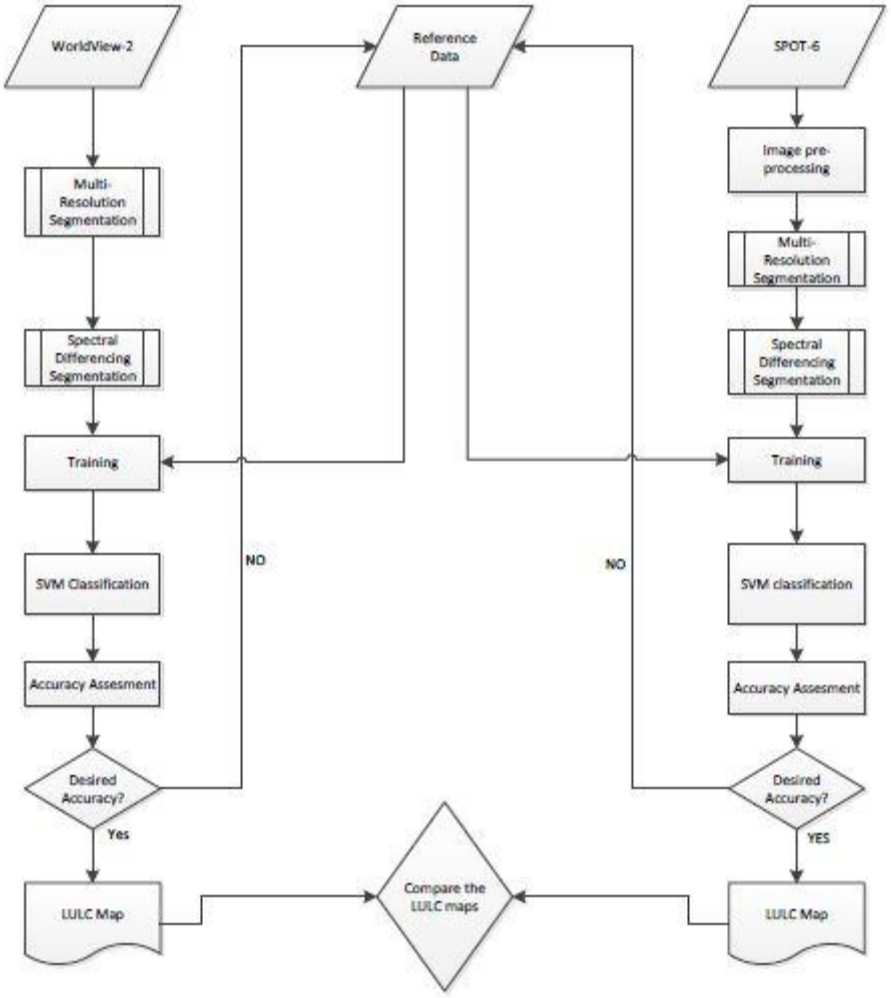

Figure 3-3: Main stages for Object-based SVM classification

3.3.6. Accuracy assessment

An accuracy statement is an important accompaniment to any thematic map derived from remote sensing, and it is generally accepted that no classification is complete until its accuracy has been thoroughly evaluated (Foody, 2002). The accuracy of a classification refers to the extent of correspondence between the remotely sensed imagery data and reference data (Iqbal and Khan, 2014). Accuracy assessment in remote sensing LULC mapping studies is essential to assess remote sensing final product. The purpose of assessment is vital to gain a warranty of classification quality and to inform the confidence of the user on the resultant product (Hasmadi *et al.*, 2009).

Accuracy assessment for classifications was done through the application of typical procedures for image classifications using confusion matrices. The overall accuracies, error producer's accuracies, user's accuracies and kappa indices for all produces maps were then evaluated. The accuracies are expressed as proportions, with the overall accuracy

representing the probability that a randomly selected point is classified correctly on the map (Foody, 2002; Adam *et al.*, 2014). The producer's accuracy is indicative of the probability that the classifier has correctly labelled in an image pixel, whereas the user's accuracy indicating the probability of this classification (Adam *et al.*, 2014). The kappa coefficient measures the difference between the actual agreement between reference data and the classifier used to perform the classification versus the likelihood of agreement between the reference data and a random classifier (Foody, 2002; Adam *et al.*, 2014). For each classification, a confusion matrix is presented, along with its kappa coefficient overall, user's and producer's accuracies. Although there is no recognized standard for accuracy assessment, a commonly suggested accuracy level is 85% (Foody, 2002).

3.4. Comparison of imagery and analysis approach performances

3.4.1. Qualitative comparison

The initial qualitative comparison was based on visual observation of the produced maps with special emphasis on the relative spatial distribution of the classes across the scene. The visual comparison was accompanied by comparison of the confusion matrices where the overall accuracies, kappa coefficients, producer's accuracies and the user's accuracies are included. The qualitative comparisons were then subjected to inference of the superiority of LULC maps generated with the different image classification approaches and imagery packages, and the statistical dependence test for the dependence of pair error matrices. The number of correctly and the incorrectly validation samples for any combination of alternatives were cross-tabulated as in Table 3-6 (de Leeuw *et al.*, 2006).

Table 3-6: Cross tabulation of number of correct and incorrectly classified pixels for the alternative classifiers/imageries

	Classifier/imagery 2	
Classifier/imagery 1	Incorrect	Correct
Incorrect	f11	f12
Correct	f21	f22

In Table 3-6, f_{12} represents the number of samples misclassified by the first classification process but correctly classified by the second, with f_{21} representing the number of samples that are correctly classified by the first classification algorithm but misclassified by the second classification algorithm (Foody, 2002; Adam *et al.*,2014). The chi-square test was

conducted in order to test the independency (H_o) of the classifications and the alternative hypothesis (H_a) of the dependency of the two classifications.

The chi-square distribution is represented by:

$$X^2=\frac{(f_{12}-f_{21})^2}{f_{12}+f_{21}}$$

and follows a z-distribution with 1 degree of freedom (Foody, 2002; de Leeuw *et al.,* 2006). The McNemar's test was used to measure: whether a statistically significant difference exists between classifications performances on the same image package using different approaches and whether a statistically significant difference exists between classifications performances on the different image package using same approaches. The McNemar's test is based on the standardized normal test expressed as by:

$$Z=\frac{f_{12}-f_{21}}{\sqrt{f_{12}+f_{21}}}$$

The difference in accuracy between the two error matrices of the classification is statistically significant ($\alpha \leq 0.05$) if the Z value is more than 1.96 (Foody, 2002; de Leeuw *et al.,* 2006; Adam *et al.,* 2014).

3.4.2. Quantitative comparisons

The quantitative comparisons involved the evaluation of the differences in terms of the area and proportions covered by each class of each classification outputs. The area in this study is expressed in hectares (ha) and proportion in percentages. The area was calculated as product of pixel counts and the spatial resolution of that particular image, i.e. pixel counts were multiplied by 36 m^2 for SPOT-6 and 4 m^2 for the WorldView-2, and then converted into hectares and proportion for each class being expressed as a percentage (%).

3.5. Analysis of the relationship between topographical variables and LULC

The distribution of LULC classes across the topographic variables was determined by thematic overlay analysis. For this purpose, the LULC map with the best accuracy (i.e. map produced from Object-based SVM on the WorldView-2) was resampled using the 30m

SRTM DEM so that its spatial resolution was 30 x 30 m. The resampled LULC map and the derived topographical variables were subjected to three separate overlay analyses. The product of these overlay analyses are presented as tables which show the occurrence of LULC types as a function of altitude, slope and aspect.

The altitude in the study area ranges between 2092 and 3036 m asl. For the LULC types and the elevation overlay analysis, the altitude was categorised into 5 classes with an interval of ~200 m. The aspect map was generated from the same SRTM with eight categories, namely: north (337.5 – 22.5°), northeast (22.5 – 67.5°), east (67.5 – 112.5°), southeast (112.5 – 157.5°), south (157.5 – 202.5°), southwest (202.5 – 247.5°), west (247.5 – 292.5°) and northwest (292.5 – 337.5°) (Wondie *et al.,* 2012). The slope map was categorised into five classes using natural jenks: 0 – 15.40°, 15.41 - 27.10°, 27.11 - 39.14°, 39.15 - 53.73° and > 53.73°.

The overlay analysis was conducted on an ArcMap 10.3 Desktop® environment (see workflow on Figure 3.4) using Raster Calculator. Each topographic variable relationship with the distribution of the LULC classes was analysed separately so that three tables depicting the distribution of each LULC classes across the different categories aspect, altitude and slope. The tables were populated with the area (ha) and proportions (%) at each category of the topographic variable which are then subjected to descriptive analysis of the trends displayed by the relationships. The descriptive analysis was conducted in order to evaluate if there has been significant conservation of topographic induced patterns in terms of the distribution of LULC types across the study area.

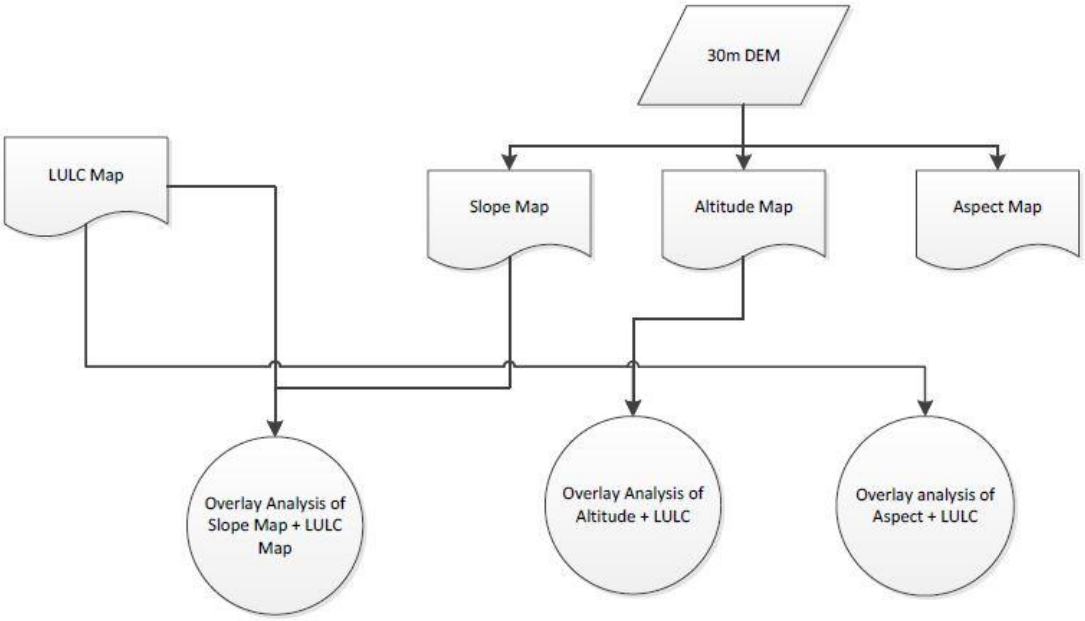

Figure 3-4: Workflow for the evaluation of the relationship between topography and LULC

4. RESULTS

4.1. Comparisons of imagery and analysis approach performances

In order to illustrate the results, a series of LULC maps is presented below i.e. Figure 4-1 to 4-4. A total of 4 maps was produced for the Mokhothlong District of Lesotho, using the combinations of the two images (WorldView-2 and SPOT-6) and the analysis approaches (PBA and OBIA) demonstrating the 9 main LULC types. The differences on the thematic maps were evaluated using three different techniques, i.e. visual examination, comparison of the quantities of each class in each map, and also the accuracy achieved by each classification as per the confusion error matrices. The statistical significance of the differences from different classification combinations was evaluated using the McNemar's tests.

4.1.1. Visual examination differences on LULC thematic maps

In general, all four maps LULC maps presented reasonably accurate visual depiction of the broad LULC types of interest in the study area. All 9 LULC types or classes were represented in each map and no pixel was left unclassified.

4.1.1.1. Comparison of image packages: SPOT-6 and WorldView-2

The first visually notable difference when comparing the imagery packages is that the SPOT-6 maps are characterised with more misclassifications compared to WorldView-2. The disparity in terms of the abundance of the misclassifications can be attributed to the difference in the imagery resolutions. SPOT-6 has relatively coarser spatial and broader spectral resolutions compared to WorldView-2 (see Table 3-1). This therefore meant that there was less detail to use during the classification of SPOT-6 than WorldView-2, which then offers a greater probability for misclassifications and class confusion on the former imagery package. The above observations are consistent with the findings of Lu et al. (2005) that higher spatial resolution offer better chances for classification accuracies and also emphasizing the significance of short-wave infrared bands in LULC classifications.

In addition to misclassifications, it is also observable that the thematic maps that involved SPOT-6 image were characterised with stronger speckle or salt-and-pepper effects which gave them "blurred" appearances compared to their WorldView-2 counterparts. The WorldView-2 thematic maps achieved relatively similar LULC types' distributions as that of the ISO Unsupervised Clustering classification on the 0.5 m pansharpened WorldView-2

used for sampling compared to SPOT-6. The above was not very surprising as the image used for sampling shares the same spectral characteristics as the WorldView-2.

The SPOT-6 faced difficulties in terms of capturing the small features and those in heterogeneous surrounding such as by the rivers where there are alternating occurrences of waterbodies, shadows, vegetation, rock outcrops and bare soil. The above problem was however was significantly overcome by the WorldView-2 due to its higher spatial and spectral resolutions.

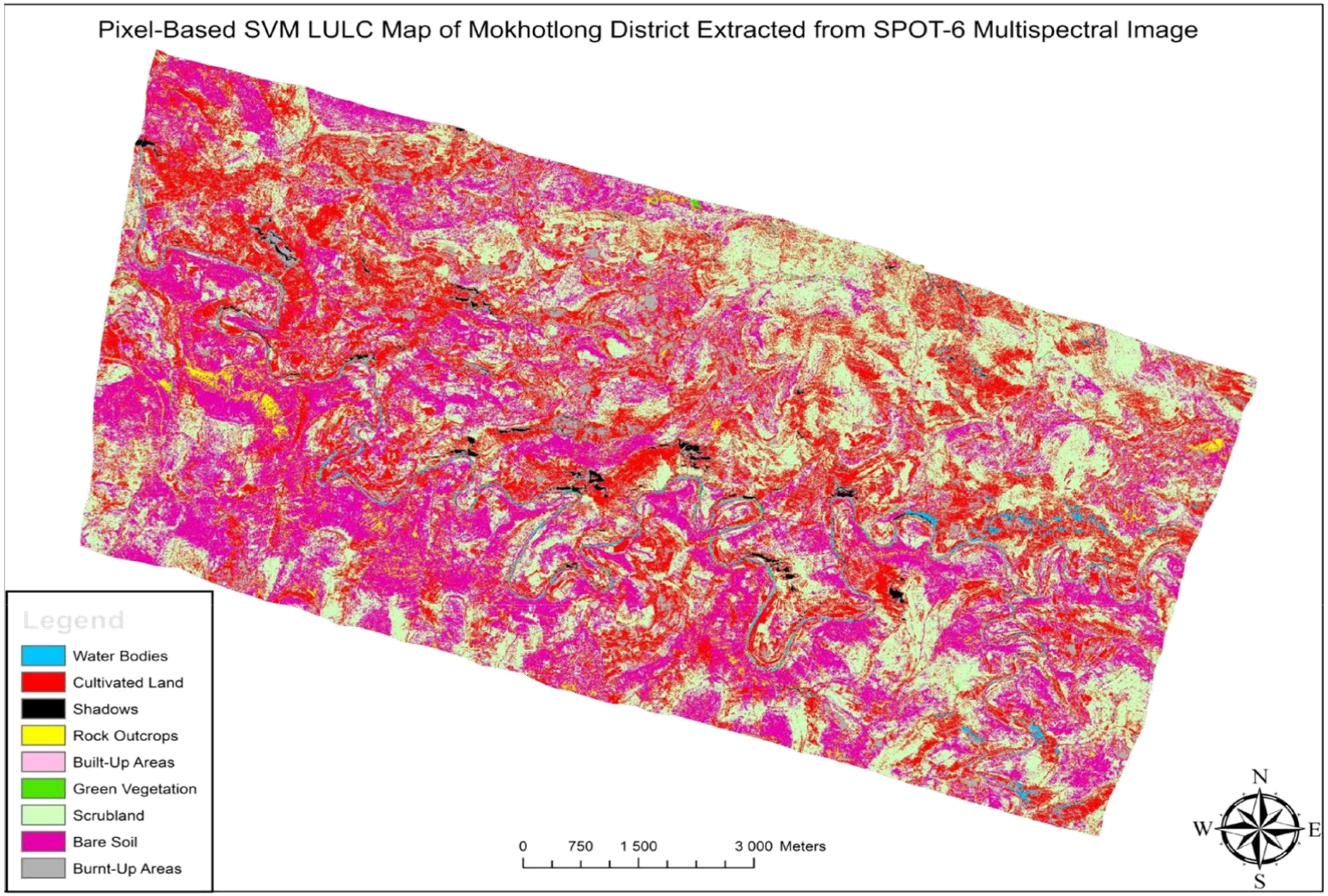

Figure 4-1: Pixel-Based SVM LULC Map of Mokhotlong District Extracted from a SPOT-6 Multispectral Image

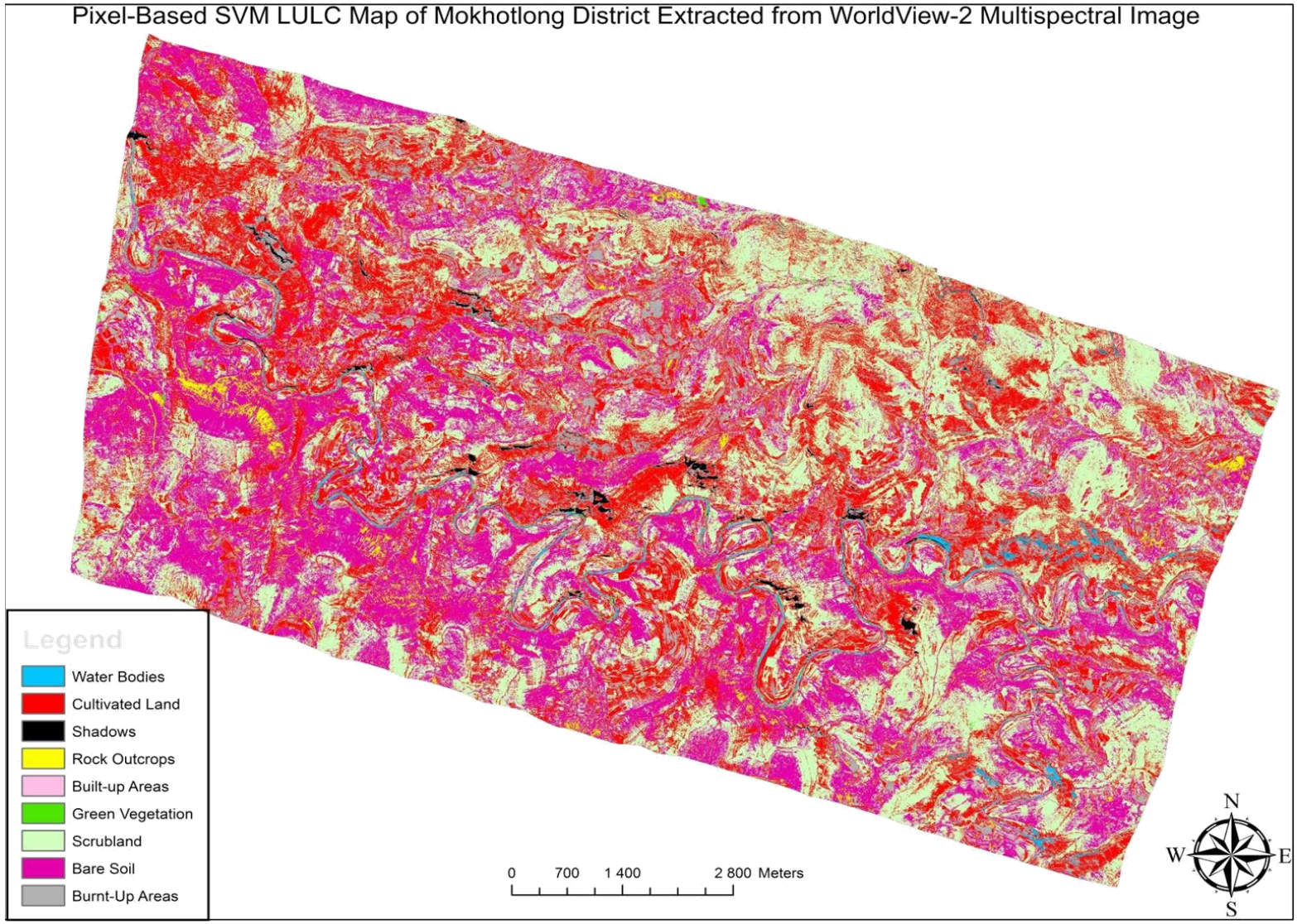

Figure 4-2: Pixel-Based SVM LULC Map of Mokhotlong District Extracted from a WorldView-2 Multispectral Image

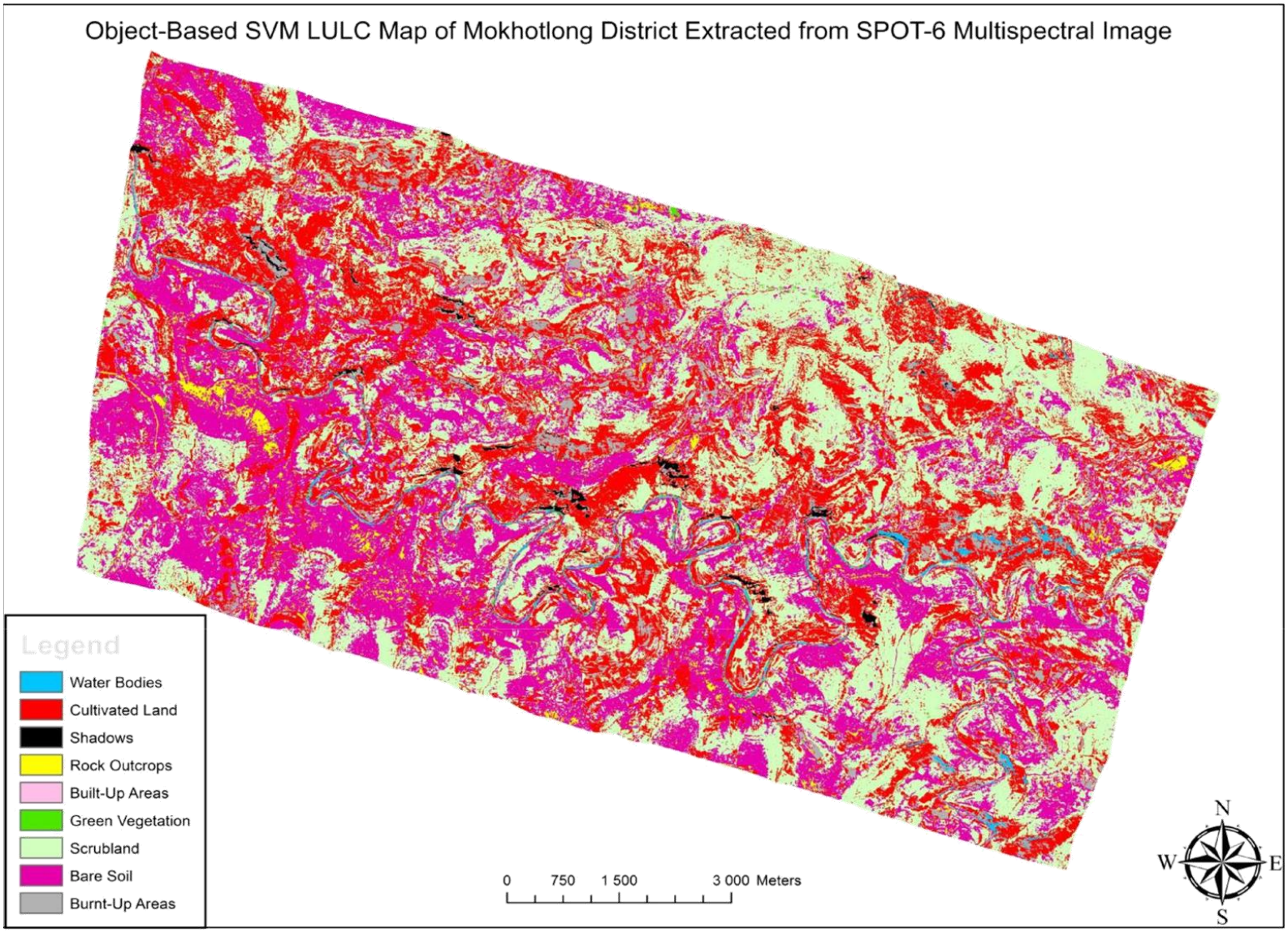

Figure 4-3: Object-Based SVM LULC Map of Mokhotlong District Extracted from a SPOT-6 Multispectral Image

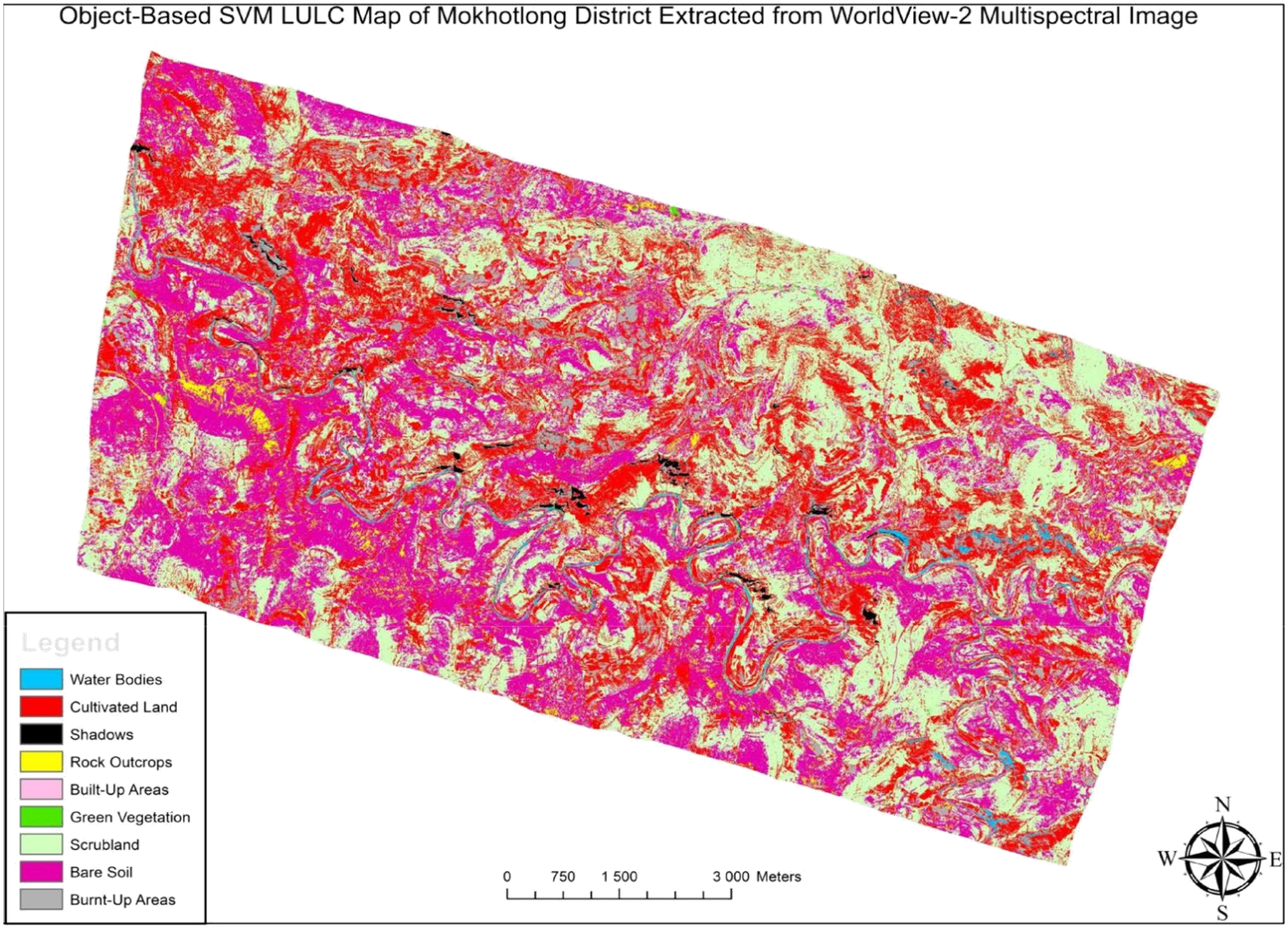

Figure 4-4: Object-Based SVM LULC Map of Mokhotlong District Extracted from a WorldView-2 Multispectral Image

4.1.1.2. Comparison of image analysis approaches: PBIA and OBIA

While both approaches produced aggregations of LULC types in the study area, the most prominent difference between the PBIA and OBIA classified thematic maps from visual inspections is that the OBIA features have more pronounced boundaries and have significantly less salt-and-pepper effects compared to those achieved from PBIA classifications. This difference can be attributed to the fact that the OBIA features are comprised on multi-pixel units and were classified as such, whereas the PBIA ones were classified as per-pixel level. Classifications at per-pixel level are more susceptible to misclassifications and confusions in PBIA than OBIA because of the fact that they only base their grouping on spectral characteristics. The above problem is more pronounced when classifying the heterogeneous regions on the imagery scene. This observation is consistent with the findings of Blaschke *et al.* (2006), Matinfar *et al.* (2007) and Bhaskaran *et al.,* (2010).

The OBIA classification approach has an advantage over PBIA by offering the opportunity to integrate spatial and spectral information into the classification which enhanced the accuracy of the thematic maps. The OBIA classification approach proved to be a very effective tool for producing LULC thematic maps of heterogeneous mountains from high resolution multispectral imageries that can visually interpreted with relative ease compared to those achieved from the PBIA approach.

4.1.2. Comparison of differences in quantities of LULC types on the different thematic maps

4.1.2.1. Comparison of SPOT-6 and WorldView-2

The quantitative evidence of the above visual observations is provided in Table 4-1 and Table 4-2, which depicts the areas (ha), proportions (%), and the differences (WorldView2 – SPOT6) of LULC achieved from the two images from the same classification approach.

As illustrated in Table 4-1, the evaluation of the differences in quantities of the LULC types revealed there are, but minor inconsistencies in terms of the relative proportions of the classes in the two images when the same PBIA SVM algorithm and training data were used. The differences are all within the confines of 2%, however when inspecting the differences in terms of area, one can notice that there had been some significant differences in classes such as the burnt areas (~165.4 ha) and cultivated area (~97.01 ha). It is worth a mention that in none of the 9 LULC types used for this study, the two images achieved the equal area as the other and that although these differences may seem minimal when looking at the area in

hectares and proportions, these differences are very significant if one is inspecting them at m^2 which defines the spatial resolutions of the used images.

Table 4-1: Areas and proportions of LULC types of WorldView-2 and SPOT-6 achieved through the PBIA SVM Classification

	WorldView-2		SPOT-6		differences	
LULC Classes	Area (ha)	Proportions (%)	Area (ha)	Proportions (%)	Area (ha)	Proportions (%)
Water Bodies	74.08	0.714	77.02	0.726	-2.94	-0.0127
Cultivated Land	2620.70	25.245	2717.71	25.626	-97.01	-0.3813
Shadows	55.14	0.531	54.19	0.511	0.95	0.0202
Rock Outcrops	181.09	1.744	155.61	1.467	25.48	0.2771
Built-Up Area	6.91	0.067	5.47	0.052	1.44	0.0150
Green Vegetation	36.24	0.349	32.96	0.311	3.28	0.0383
Scrubland	4080.10	39.303	4099.52	38.655	-19.42	0.6473
Bare Soil	2833.07	27.290	2803.57	26.435	29.50	0.8548
Burnt Areas	493.93	4.758	659.29	6.217	-165.36	-1.4587
	10381.24	100.000	10605.33	100.000		

These differences may be attributed to the fact that the analyses used for this study are susceptible to salt-and-pepper effects which then can lead to misclassifications and confusion in heterogeneous parts of the scene. These class confusions and misclassifications are then translated to the differences in the resultant areas and proportions. The two above phenomena may not necessarily occur at the same sets of pixels and for the same LULC classes, because if that was the case, there would not necessarily be any difference in the areas as the errors would just cancel each other out. Here even though the same set of training samples and classification algorithms were used, the images are characterised with different spatial and spectral resolutions (Table 3-1) which therefore reveals that the differences in both resolutions characterising the images has an effect on the results.

Table 4-2: Areas and proportions of LULC types of WorldView-2 and SPOT-6 achieved through the OBIA SVM Classification

	WorldView-2		SPOT-6		differences	
LULC Classes	Area (ha)	Proportions (%)	Area (ha)	Proportions (%)	Area (ha)	Proportions (%)
Water Bodies	80.12	0.772	80.41	0.774	-0.29	-0.0028
Cultivated Land	2645.94	25.482	2646.40	25.486	-0.46	-0.0043
Shadows	59.06	0.569	59.08	0.569	-0.02	-0.0002
Rock Outcrops	220.14	2.120	219.11	2.110	1.03	0.0100
Built-Up Area	9.39	0.090	9.26	0.089	0.13	0.0013
Green Vegetation	40.37	0.389	40.47	0.390	-0.10	-0.0010
Scrubland	4042.46	38.932	4042.65	38.933	-0.19	-0.0016
Bare Soil	2764.94	26.628	2765.58	26.634	-0.64	-0.0060
Burnt Areas	521.08	5.018	520.62	5.014	0.47	0.0045
TOTALS	10383.51	100.000	10383.58	100.000		

Table 4-2 presents the results of the evaluation of the differences in quantities of the LULC types on WorldView-2 and SPOT-6 images when the same sets of training data and object-based SVM classifier were used. The table shows that there had been substantial reductions in terms of the differences compared to when the same images were used in the PBIA approach. This may be attributed to the fact that pixels were grouped into image objects during the two segmentation techniques, as per their similar spatial and spectral characteristics, such that chances for confusions and misclassification had been considerably reduced.

4.1.2.2. Comparison of image analysis approaches: PBIA and OBIA

Largely, both classification approaches enabled a reasonably similar visual depiction of broad LULC types of interest in the study area on both images, although there were some visually observed differences particularly those to do with the abundance of the salt-and-pepper effects. The quantitative evidence of the above visual observations is provided in Table 4-3 and Table 4-4, which depict the areas (ha), proportions (%), and the differences (PBIA – OBIA) of LULC achieved from the two images from the different classification approaches.

Table 4-3: Areas and proportions results achieved from OBIA and PBIA approaches on SPOT-6 imagery

	OBIA		PBIA		differences	
LULC Classes	Area (ha)	Proportions (%)	Area (ha)	Proportions (%)	Area (ha)	Proportions
Water Bodies	77.02	0.726	80.41	0.774	-3.39	-0.048
Cultivated Land	2717.71	25.626	2646.40	25.486	71.31	0.139
Shadows	54.19	0.511	59.08	0.569	-4.89	-0.058
Rock Outcrops	155.61	1.467	219.11	2.110	-63.50	-0.643
Built-Up Area	5.47	0.052	9.26	0.089	-3.79	-0.038
Green Vegetation	32.96	0.311	40.47	0.390	-7.52	-0.079
Scrubland	4099.52	38.655	4042.65	38.933	56.87	-0.278
Bare Soil	2803.57	26.435	2765.58	26.634	37.99	-0.199
Burnt Areas	659.29	6.217	520.62	5.014	138.67	1.203
	10605.33	100.000	10383.58	100.000		

Table 4-3 presents the evaluation of the differences in the quantities of the 9 LULC classes used as classified using the OBIA and PBIA analysis approaches on the same SPOT-6 multispectral image. The differences in the two are similar to those when the different images were compared using the same classifications. The differences were all below 1% except for the burnt area class where the difference was just above 1.2%. As in the previous comparisons, the use of the proportional difference can be deceiving, the differences in the areas in ha shows that there were differences for classes such as burnt areas (~138.7 ha), cultivated areas (71.3 ha), rock outcrops (~63.5 ha) and scrubland (~56.9 ha). These differences may look negligible when just looking at them in hectares and percentages but are quite significant at the units of the spatial resolutions of the images.

The differences in the quantities of the classes achieved through the different classification approaches on the same imagery using the same classification algorithm and training data may be attributed to the fact that the analyses base the classification on different units. The OBIA approach clusters pixels prior classification on the basis of their similarities in terms of their spectral and spatial characteristics whereas the PBIA classify pixels at individual level, which makes them very vulnerable to misclassifications and class confusions during classifications (Blaschke *et al.*, 2006).

Table 4-4: Areas and proportions results achieved from OBIA and PBIA approaches on WorldView-2 imagery

	OBIA		PBIA		differences	
LULC Classes	Area (ha)	Proportions (%)	Area (ha)	Proportions (%)	Area (ha)	Proportions
Water Bodies	74.08	0.714	80.12	0.772	-6.05	-0.058
Cultivated Land	2620.70	25.245	2645.94	25.482	-25.24	-0.238
Shadows	55.14	0.531	59.06	0.569	-3.92	-0.038
Rock Outcrops	181.09	1.744	220.14	2.120	-39.05	-0.376
Built-Up Area	6.91	0.067	9.39	0.090	-2.48	-0.024
Green Vegetation	36.24	0.349	40.37	0.389	-4.14	-0.040
Scrubland	4080.10	39.303	4042.46	38.932	37.64	0.371
Bare Soil	2833.07	27.290	2764.94	26.628	68.13	0.662
Burnt Areas	493.93	4.758	521.08	5.018	-27.16	-0.261
	10381.24	100.000	10383.51	100.000		

Table 4-4 presents results of the OBIA and PBIA classifications on the WorldView-2 multispectral images as well as their differences. The differences on the WorldView-2 had significantly reduced compared to those found during the comparisons using SPOT-6 (see Table 4-3). If inspecting the differences in terms of proportions (%), the notable ones includes bare soil (~0.662%), rock outcrops (~0.376%) and scrubland (~0.371%). These differences were all under 100 ha which is a similar difference compared to the differences in SPOT-6 (Table 4-3).

The differences in the quantities of the classes achieved through the PBIA and OBIA classification approaches on the same image, training dataset and algorithm may be attributed to the fact that the analyses base the classification on different units. The OBIA approach groups pixels prior classification on the basis of their similarities in terms of their spectral and spatial characteristics whereas the PBIA classify pixels at individual level which makes them very vulnerable to misclassifications and class confusions during classifications.

4.1.3. Comparison of the classification accuracies

In order to illustrate the performances of each combination of imagery and analysis approach, a series of error matrices with the producer's and user's accuracies for the classifications is presented in Table 4-5 to 4-8.

Table 4-5: Confusion matrix for the LULC classification on a SPOT-6 image using a PBIA approach

	Classification Data												
Reference Data	**LULC CLASSES**	Bare Soil	Water Bodies	Cultivated Land	Shadows	Rock Outcrops	Built-Up Areas	Green Vegetation	Scrubland	Burnt areas	TOTALS	omissions	Producer's accuracy (%)
	Bare Soil	19	0	2	0	3	2	0	0	0	**26**	7	73.1
	Water Bodies	0	18	1	3	0	2	0	0	2	**26**	8	69.2
	Cultivated Land	0	0	23	0	0	0	0	3	0	**26**	3	88.5
	Shadows	0	2	0	23	0	0	0	0	1	**26**	3	88.5
	Rock Outcrops	3	0	3	0	20	0	0	0	0	**26**	6	76.9
	Built-Up Areas	1	0	0	0	2	23	0	0	0	**26**	3	88.5
	Green Vegetation	0	1	0	0	0	0	20	3	2	**26**	6	76.9
	Scrubland	1	0	4	0	0	0	2	19	0	**26**	7	73.1
	Burnt areas	0	0	3	0	0	0	0	2	21	**26**	5	80.8
	TOTALS	**24**	**21**	**36**	**26**	**25**	**27**	**22**	**27**	**26**	**234**	**48**	
	commissions	5	3	13	3	5	4	2	8	5	**48**		
	User's accuracy (%)	79.2	85.7	63.9	88.5	80.0	85.2	90.9	70.4	80.8			

Table 4-5 presents a confusion matrix for the LULC classification of Mokhotlong District on SPOT-6 using a pixel-based SVM algorithm. Table 4-5 shows that of the 234 validation samples used, 48 were misclassified or confused for a different class or the other. None of the 9 classes had all validation samples which were all classified for the in classes, but classes such as cultivated land, shadows and built-up areas were able to have 23/26 samples correctly classified, which interpreted to a 88.5% producer's accuracy. The water bodies class had the least number of validation samples correctly classified (18/26), with a producer's accuracy of 69.2%. The green vegetation class achieved the highest user's accuracy with 90.9% where it had 20 correctly classified samples and only 2 from the scrubland class.

The confusion matrix revealed that the most confusion in the classification were with the water bodies followed by the bare soil and dry vegetation LULC classes. Water bodies were mostly confused for shadows and built-up areas whereas the bare soil had been misclassified for rock outcrops, built-up area and cultivated land, and the burnt vegetation being misclassified for cultivated land and scrubland. The confusion may be attributed to the fact that these classes occurred mostly in close proximity to one another and may have shared some degrees of spectral similarities, or may have fallen on different pixels due to the difference in the resolutions of the imagery used for sampling and classification.

Table 4-6: Confusion matrix for the LULC classification on a WorldView-2 image using a PBIA approach

	Classification Data												
Reference Data	LULC CLASSES	Bare Soil	Water Bodies	Cultivated Land	Shadows	Rock Outcrops	Built-Up Areas	Green Vegetation	scrubland	Burnt areas	**TOTALS**	omissions	Producer's accuracy (%)
	Bare Soil	21	0	2	0	2	1	0	0	0	**26**	5	80.8
	Water Bodies	0	19	1	2	0	2	0	0	2	**26**	7	73.1
	Cultivated Land	0	0	24	0	0	0	0	2	0	**26**	2	92.3
	Shadows	0	2	0	23	0	0	0	0	1	**26**	3	88.5
	Rock Outcrops	3	0	1	0	22	0	0	0	0	**26**	4	84.6
	Built-Up Areas	1	0	0	0	2	23	0	0	0	**26**	3	88.5
	Green Vegetation	0	1	0	0	0	0	20	3	2	**26**	6	76.9
	scrubland	1	0	4	0	0	0	1	20	0	**26**	6	76.9
	Burnt areas	0	0	3	0	0	0	0	1	22	**26**	4	84.6
	TOTALS	**26**	**22**	**35**	**25**	**26**	**26**	**21**	**26**	**27**	**234**	**40**	
	commissions	5	3	11	2	4	3	1	6	5	**40**		
	User's accuracy (%)	80.8	86.4	68.6	92.0	84.6	88.5	95.2	76.9	81.5			

Table 4-6 presents a confusion matrix for the LULC classification of Mokhotlong District on WorldView-2 using a pixel-based SVM learning algorithm. Table 4-6 reveals that 40 out of 234 validation samples were incorrectly classified. The cultivated land class had the most validation samples correctly classified, i.e. 24/26, which is approximately ~92.3% of producer's accuracy. The shadows and built-up areas achieved the same producer's accuracy as on the previous SPOT-6 PBIA classification (~88.5%). The water bodies LULC class achieved the lowest producer's accuracy at 19/26 (~73.1%) but was higher than that from the previous classification. The cultivated land had the lowest user's accuracy at 68.6%, having at least 11 samples that had been mistaken for it. The green vegetation LULC type achieved the highest user's accuracy at ~95.2%.

The above confusions may be attributed to the close spacing of different samples. Due to the spectrally heterogeneous nature of the study area, those classes may have shared some degree of spectral similarities or may have fallen on different pixels due to the difference in the resolutions of the imagery used for sampling and classification. However, there had been some improvement in terms of classification accuracies on the WorldView-2 when compared to the same classification on SPOT-6.

Table 4-7: Confusion matrix for the LULC classification on a SPOT-6 image using an OBIA approach

	Classification Data												
Reference Data	**LULC Classes**	Bare Soil	Water Bodies	Cultivated Land	Shadows	Rock Outcrops	Built-Up Areas	Green Vegetation	scrubland	Burnt areas	TOTALS	omissions	Producer's accuracy (%)
	Bare Soil	22	0	1	0	2	1	0	0	0	**26**	4	84.6
	Water Bodies	0	21	0	3	1	0	0	0	1	**26**	5	80.8
	Cultivated Land	0	0	24	0	0	0	0	2	0	**26**	2	92.3
	Shadows	0	1	0	25	0	0	0	0	0	**26**	1	96.2
	Rock Outcrop	1	0	1	0	24	0	0	0	0	**26**	2	92.3
	Built-Up Areas	0	0	0	0	1	25	0	0	0	**26**	1	96.2
	Green Vegetation	0	0	0	0	0	0	25	1	0	**26**	1	96.2
	Scrubland	0	0	4	0	0	0	1	21	0	**26**	5	80.8
	Burnt areas	0	0	2	0	0	0	0	1	23	**26**	3	88.5
	TOTALS	**23**	**22**	**32**	**28**	**28**	**26**	**26**	**25**	**24**	**234**	**24**	
	commissions	1	1	8	3	4	1	1	4	1	**24**		
	User's accuracy (%)	95.7	95.5	75.0	89.3	85.7	96.2	96.2	84.0	95.8			

Table 4-7 presents a confusion matrix for the LULC classification of Mokhotlong District on SPOT-6 using an object-based SVM algorithm. The above confusion matrix reveals that 24/234 samples were incorrectly classified. Most misclassification in the water bodies and the scrubland classes where 21/26 samples had been correctly classified. The above LULC classes achieved the lowest producer's accuracies at ~80.8%. The cultivated land like on the previous classification achieved the lowest user's accuracy (75%) having had most number of the samples from other classes being confused with it. The highest user's accuracy was scored by the built-up areas and green vegetation LULC class at ~96.2%.

The object-based SVM classification of SPOT-6 improved the results when compared to the previous classifications presented in Table 4-5 and Table 4-6. These enhancements in classification accuracy confusions may be ascribed to the fact that OBIA classifications are conducted on multi-pixel segments rather than on individual rather as on the previous classifications. The use of multi-pixel segments image objects which share similar spectral and spatial characteristics rather than pixels as individual lessens the chances of misclassifications, as bigger and fewer units are in this case subjected to classification.

Table 4-8: Confusion matrix for the LULC classification on a WorldView-2 image using an OBIA approach

	Classification Data											
Reference Data	LULC CLASSES	Bare Soil	Water Bodies	Cultivated Land	Shadows	Rock Outcrops	Built-Up Areas	Green Vegetation	Low lying Vegetation	Burnt areas	TOTALS	omissions	Producer's accuracy (%)
	Bare Soil	23	0	1	0	1	1	0	0	0	**26**	3	88.5
	Water Bodies	0	24	0	2	0	0	0	0	0	**26**	2	92.3
	Cultivated Land	0	0	25	0	0	0	0	1	0	**26**	1	96.2
	Shadows	0	1	0	25	0	0	0	0	0	**26**	1	96.2
	Rock Outcrops	0	0	0	0	25	1	0	0	0	**26**	1	96.2
	Built-Up Areas	0	0	0	0	0	26	0	0	0	**26**	0	100
	Green Vegetation	0	0	0	0	0	0	25	1	0	**26**	1	96.2
	Low-lying Vegetation	0	0	2	0	0	0	1	23	0	**26**	3	88.5
	Burnt areas	0	0	2	0	0	0	0	2	22	**26**	4	84.3
	TOTALS	**23**	**25**	**30**	**27**	**26**	**28**	**26**	**27**	**22**	**234**	**16**	
	commissions	0	1	5	2	1	2	1	4	0	**16**		
	User's accuracy (%)	100	96.0	83.3	92.6	96.2	92.7	96.2	85.2	100			

Table 4-8 presents the confusion matrix for the accuracy assessment of the object-based SVM LULC classification on WorldView-2 image. In this classification, 16 of the 234 validations were only incorrectly classified. The built-up areas LULC classes achieved a 26/26 (100%) producer's accuracy, with other four LULC classes (cultivated land, shadows, green vegetation and rock outcrops) with just 1/26 sample being wrongly classified. The bare soil and burnt areas classes achieved 100% user's accuracy. The increased spectral and spatial resolutions of WorldView-2 and the use of the OBIA approach for the above classifications can be stated as a reason for the improvements in classifications as compared to the previous classifications.

4.1.3.1. ***Comparison of overall classifications and kappa statistics***

Table 4-9: Kappa and Overall accuracies values for the LULC classification models

	PBIA		OBIA	
Overall accuracy statistics	SPOT-6	WorldView-2	SPOT-6	WorldView-2
Kappa Coefficient	0.776	0.813	0.888	0.925
Accuracies	79.5	82.9	89.7	93.2

Table 4-9 presents the overall accuracy assessment statistics for the four LULC classification models for a sample of 234 validation samples. The comparison of the overall

accuracies and kappa coefficients for the four models reveals that there are differences in the scores of the models. When comparing the overall accuracies of the models that used the same imageries but different analysis approaches, it is discovered that the difference was ~10.2% and ~10.3% for SPOT-6 and WorldView-2, respectively. WorldView-2 enabled better classification accuracy compared to the SPOT-6 in both the PBIA and OBIA approaches.

The comparison of the overall accuracy statistics for the same classification approaches using different images revealed that the difference was 3.4% and 3.5% for the PBIA and OBIA approaches, respectively. The OBIA approach enabled better classification accuracy compared to the PBIA in both images used for this study. If using the guidance of Foody (2002) that only overall accuracy of above 85% is acceptable for application purposes, only the object-based SVM LULC models met the required minimum standard. All the four models were able to score very good overall kappa statistics, as the lowest kappa value fell in the category which is considered as showing a good agreement, and the rest were in the very good agreement category.

4.1.3.2. *Evaluation of the statistical significance of the difference in classification accuracies*

Tables 4-10 to 4-13 are the cross-tables presenting the error matrices of the correctly and incorrectly pixels/objects in the conducted classification processes.

Table 4-10: Frequency of correct and incorrectly classified pixels by PBIA on SPOT-6 and WorldView-2

PBIA	**WORLDVIEW-2**		
SPOT 6	Incorrect	Correct	Total
Incorrect	32	16	48
Correct	8	178	186
Total	40	194	234

Table 4-10 shows the number of pixels correctly and incorrectly classified on the PBIA classification on SPOT-6 (Table 4-5) and WorldView-2 (Table 4-6). The table indicates that the two classifications agreed on 210 pixels, with 178 correctly classified on both classifications and 32 incorrect on both classifications. The classifiers failed to agree on 24 out of 234 pixels, as shown on the top right and bottom left diagonal. The chi-squared test was conducted in order to evaluate the independency of Table 4-5 and Table 4-6. The null hypothesis states of this test stated that that knowing the accuracy level of Table 4-5 cannot

help one to predict the level of Table 4-6 and vice-versa, i.e., the two matrices are independent. In simple form, the

H_0: Table 4-5 and Table 4-6 are independent.

H_a: Table 4-5 and Table 4-6 are not independent

$\alpha = 0.05$

The chi-square value of Table 4-10 equals to 104.71, with a p-value of >0000.1 at $\alpha = 0.05$. This reveals the lack of independence in the data represented in the matrix, rejecting the null hypothesis. Thus we can accept the alternative hypothesis, which states that the data presented on the two confusion matrices are dependent on one another. The McNemar's test statistic of Table 4-10 is equal to 2.632 thus greater than 1.96. This therefore implies that the difference between the performances of SPOT-6 and WorldView-2 when PBIA statistically significant at 95% significance level.

Table 4-11: Frequency of correct and incorrectly classified pixels by OBIA on SPOT-6 and WorldView-2

OBIA	**WORLDVIEW-2**		
SPOT 6	Incorrect	Correct	Total
Incorrect	12	4	16
Correct	12	206	218
Total	24	210	234

Table 4-11 shows the number of pixels correctly and incorrectly classified on the OBIA classification on SPOT-6 (Table 4-7) and WorldView-2 (Table 4-8). The table indicates that the two classifications agreed on 218 pixels, with 206 correctly classified on both classifications and 12 incorrect on both classifications. The classifiers failed to agree on 16 out of 234 pixels, as shown on the top right and bottom left diagonal. The chi-squared test was conducted in order to evaluate the independency of Table 4-7 and Table 4-8. The null hypothesis states of this test stated that that knowing the accuracy level of Table 4-7 cannot help one to predict the level of Table 4-8 and vice-versa, i.e., the two matrices are independent.

The chi-square value of Table 4-11 equals to 78.21, with a p-value of >0000.1 at $\alpha = 0.05$. This reveals the lack of independence in the data represented in the matrix. Hence, the null hypothesis is rejected and the alternative hypothesis is accepted, which states that the data presented on the two confusion matrices are dependent samples. The McNemar's test statistic of the above matrix is 2 and is greater than 1.96. This therefore reveals that the

difference between the performances of SPOT-6 and WorldView-2 when SVM is applied through an OBIA approach is applied is statistically significant at 95% significance level.

Table 4-12: Frequency of correct and incorrectly classified objects on SPOT-6 by PBIA and OBIA approaches

SPOT-6	*OBIA*		
PBIA	Incorrect	Correct	Total
Incorrect	12	36	48
Correct	12	174	186
Total	24	210	234

Table 4-12 presents the number of pixels correctly and incorrectly classified on the through the PBIA (Table 4-5) and OBIA (Table 4-7) on the SPOT-6 multispectral image. The above Table 4-12 stipulates that the two classifications processes agreed on 186 pixels of which 174 are correctly classified and 12 incorrectly classified. The classifiers failed to agree on 48 out of 234 pixels, as shown on the top right and bottom left diagonal. The chi-square value of Table 4-11 is 14.2611. The p-value is 0.000159. This result is significant at $p < 0.05$. This reveals the lack of independence in the data represented in the matrix. Thus reject the null hypothesis and accept the alternative hypothesis, which states that the data presented on the two confusion matrices are dependent samples.

The McNemar's test statistic of the above matrix is equal to 3.46 and is greater than 1.96. This therefore reveals that the difference between the performances of the SVM classifier through the PBIA and OBIA on SPOT-6, are statically significantly at 95% significance level.

Table 4-13: Frequency of correct and incorrectly classified objects on WorldView-2 by PBIA and OBIA approaches

WorldView-2	*OBIA*		
PBIA	Incorrect	Correct	Total
Incorrect	10	30	40
Correct	6	188	194
Total	16	218	234

Table 4-13 presents the number of pixels correctly and incorrectly classified on the through the PBIA (Table 4-6) and OBIA (Table 4-8) on the WorldView-2 multispectral image. The two classifiers agreed on 198 sample pixels and failed to agree on 36 out of 234 pixels, as shown on the top right and bottom left diagonal. The chi-square statistic is 24.9848. The p-value is .000001. This result is significant at $p < 0.05$. This reveals the lack of independence in the data represented in the matrix, so the null hypothesis is rejected and accept the alternative hypothesis. The McNemar's test statistic of the above matrix is equal to 3.53 and is greater than 1.96. This therefore reveals that the difference between the performances of the SVM classifier through the PBIA and OBIA on SPOT-6, are statistically significantly at 95% significance level.

4.2. The relationship between LULC distribution and topography in the study area

The classification model involving the WorldView-2 and the object-based SVM learning algorithm achieved the highest overall accuracy statistics with an accuracy of 93.2% and kappa coefficient of 0.925. This therefore meant that the thematic map from the above classification model was to be used for the overlay analysis with the DEM derived topographic variable maps of elevation, slope and aspect in order to assess the relationship between LULC spatial distribution and topography.

Figures 4-7 to 4-9 presents the elevation, slope and aspect maps of the study area derived from an SRTM DEM with the spatial resolution of 30 m. The LULC map was resampled to cell sizes of the topographical variable maps, so that they're subjected to overlay analysis. This therefore meant that the spatial resolution of the LULC maps was decreased from 2 m to 30 m.

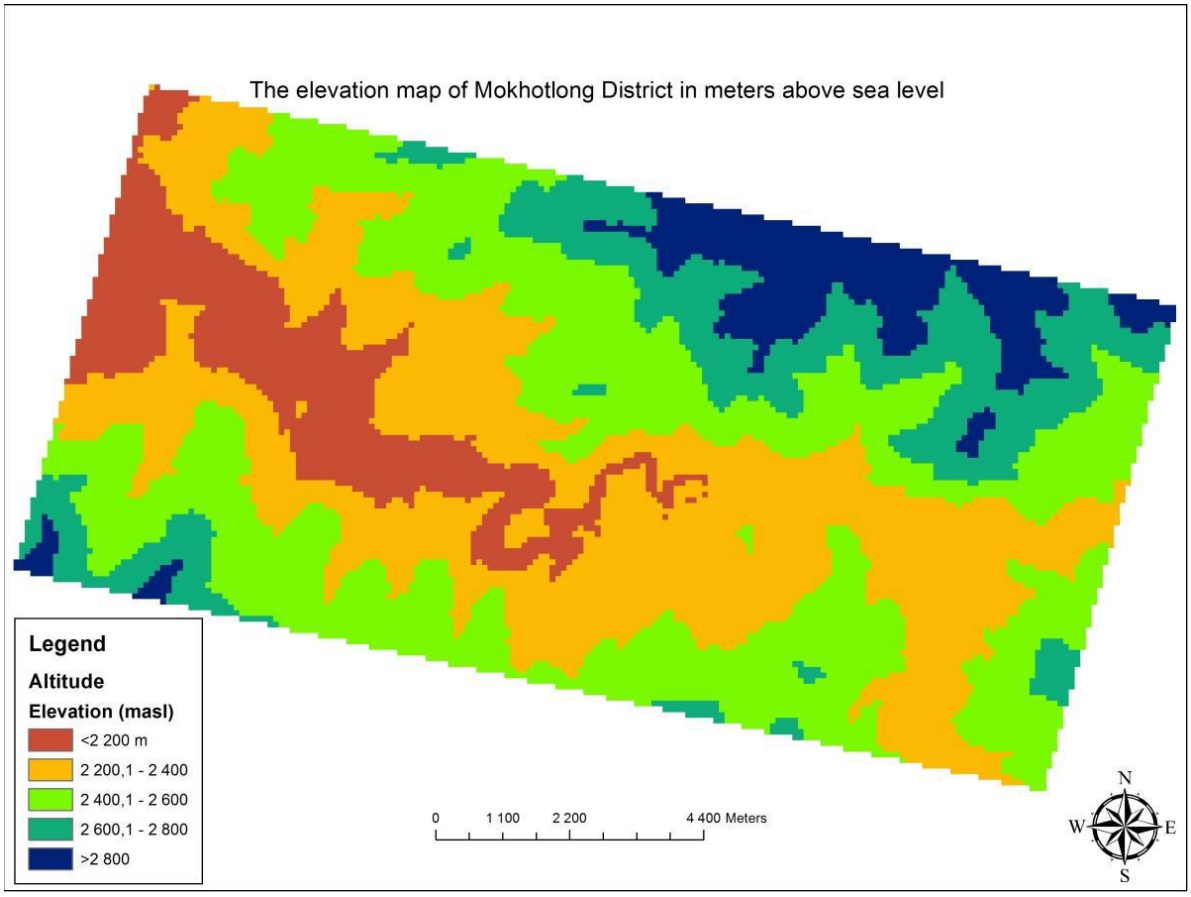

Figure 4-5: The elevation map of the study area at 30 m resolution

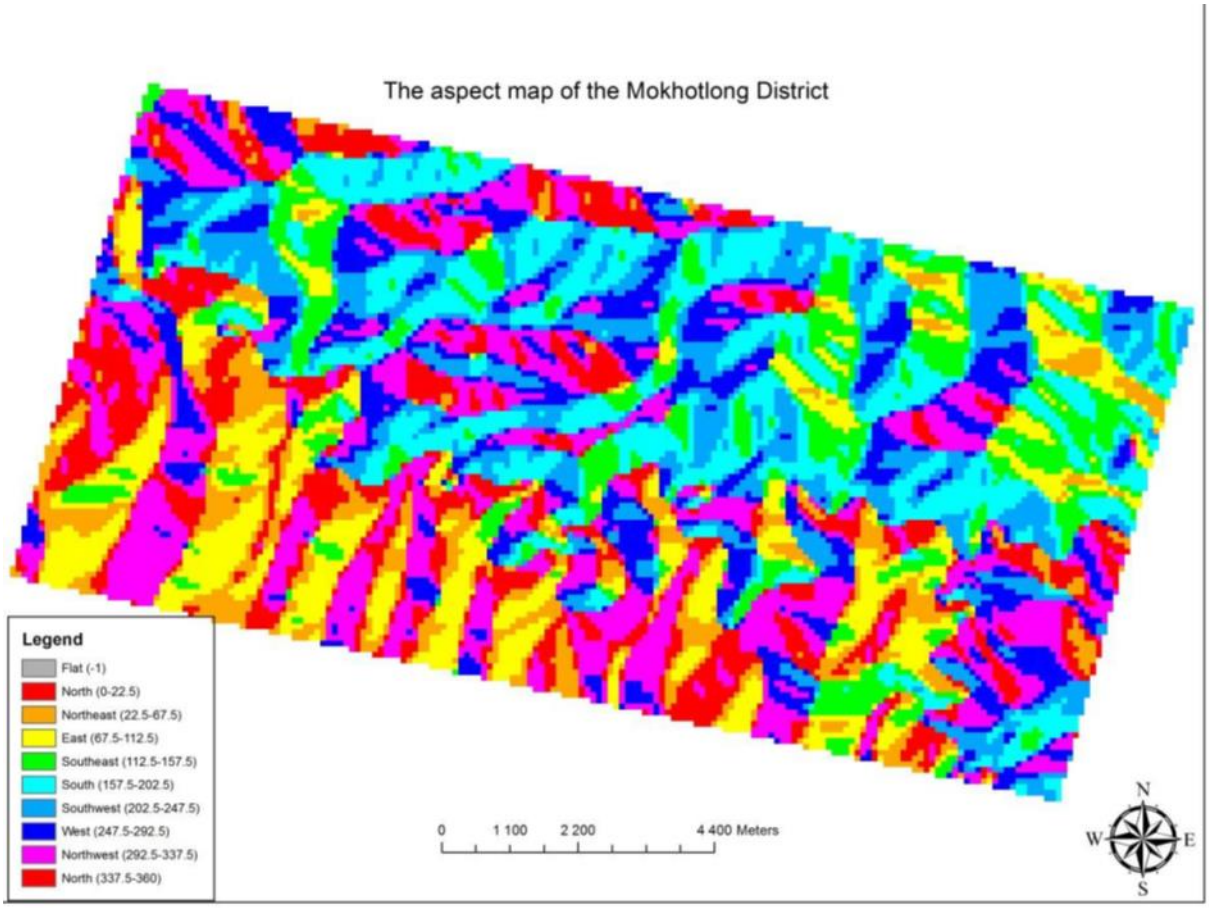

Figure 4-6: The aspect map of the study area at 30 m resolution

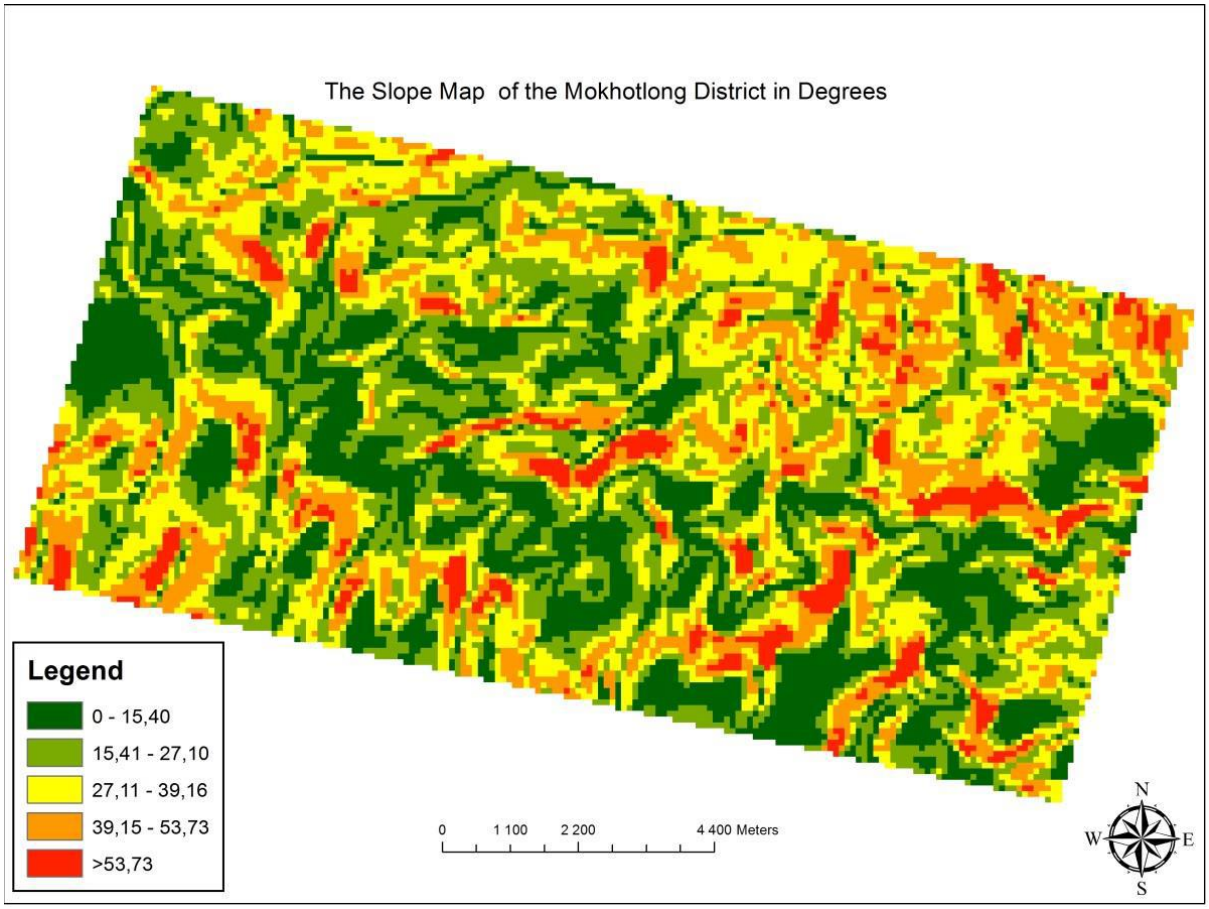

Figure 4-7: The slope map of the study area at 30 m resolution

4.2.1. LULC distribution and elevation

Table 4-14: Extent of the altitudinal ranges across the study area and distribution of LULC classes within each altitudinal range

LULC Types		ALTITUDINAL RANGE (m asl)					TOTAL
		<2200	2200-2400	2400-2600	2600-2800	>2800	
Water Bodies	Area (ha)	26.52	39.78	19.16	1.47	4.42	91.36
	Proportion (%)	0.26	0.38	0.18	0.01	0.04	0.88
Cultivated Land	Area (ha)	372.05	1028.49	837.67	294.70	125.25	2658.15
	Proportion (%)	3.58	9.90	8.07	2.84	1.21	25.60
shadows	Area (ha)	5.89	30.94	8.10	3.68	5.16	53.78
	Proportion (%)	0.06	0.30	0.08	0.04	0.05	0.52
Rock outcrops	Area (ha)	25.79	123.04	59.68	18.42	0.74	227.65
	Proportion (%)	0.25	1.18	0.57	0.18	0.01	2.19
Built-up areas	Area (ha)	2.95	6.63	1.47	0.00	0.00	11.05
	Proportion (%)	0.03	0.06	0.01	0.00	0.00	0.11
Green vegetation	Area (ha)	5.89	10.31	4.42	5.16	3.68	29.47
	Proportion (%)	0.06	0.10	0.04	0.05	0.04	0.28
Scrubland	Area (ha)	404.47	1226.67	1449.16	651.28	333.74	4065.32
	Proportion (%)	3.90	11.81	13.96	6.27	3.21	39.15
Bare Soil	Area (ha)	433.94	1270.87	829.57	165.77	36.10	2736.24
	Proportion (%)	4.18	12.24	7.99	1.60	0.35	26.35
Burnt areas	Area (ha)	55.26	193.03	201.87	41.26	19.16	510.56
	Proportion (%)	0.53	1.86	1.94	0.40	0.18	4.92
TOTAL	Area (ha)	1345.06	3965.75	3442.00	1192.71	533.14	10478.66
	Proportion (%)	12.84	37.85	32.85	11.38	5.09	100

Table 4-14 presents the areas and proportions of LULC types occurring in the study area across the defined elevation ranges. The elevation was categorised into 5 classes with ranges of ~200 m above sea level (asl). According to Wondie *et al.* (2012) elevation plays an important role in terms of the determination of life, particularly the distribution of primary productivity and is a typical characteristic of mountainous regions. The study area exists between the elevations of just below 2000 to just over 3000 m asl with an average of about 2300 m asl (see Figure 4-5). The 2201 – 2400 m and 2401 – 2600 m asl ranges cover about 37.851% and 32.85%, respectively to the total area. The three remaining elevation ranges cover the remaining balance, with the >2800 m class covering the least proportion of the study area (~533.14 ha).

All LULC classes identified in this study existed in all of the 5 elevation categories except for the built-up areas which did not exist in the 2600-2800 and >2800 m asl categories. The absence of built-up areas in higher areas may be due to the fact that in those elevation ranges it might be too cold for human to settle as temperature is known to decrease with increasing altitude and also remoteness to water bodies, pastures and agricultural land. The general trend of the distribution of most LULC types with respect to elevation is that they increased with altitude from <2200 m asl to 2201 – 2400 m asl, and then declined from thereon except for the scrubland and burnt areas which only started their abrupt decline from the 2401 – 2600 m asl.

4.2.2. LULC distribution across slope

Table 4-15: Spatial distribution of LULC types across slopes categories, their totals and percentage area coverages in the study area

LULC Types	Slope (degrees)						
		0-15.40	15.41 - 27.10	27.11-39.16	39.15-53.73	>57.73	Total
Water Bodies	Area (ha)	25.05	22.84	14.00	14.73	14.73	91.36
	Proportion (%)	0.24	0.22	0.13	0.14	0.14	0.88
Cultivated Land	Area (ha)	582.76	679.27	668.22	533.40	194.50	2658.15
	Proportion (%)	5.61	6.54	6.44	5.14	1.87	25.60
shadows	Area (ha)	1.47	3.68	11.79	11.05	25.79	53.78
	Proportion (%)	0.01	0.04	0.11	0.11	0.25	0.52
Rock outcrops	Area (ha)	80.30	78.83	53.05	13.26	2.21	227.65
	Proportion (%)	0.77	0.76	0.51	0.13	0.02	2.19
Built-up areas	Area (ha)	4.42	5.16	1.47	0.00	0.00	11.05
	Proportion (%)	0.04	0.05	0.01	0.00	0.00	0.11
Green vegetation	Area (ha)	10.31	9.58	5.16	3.68	0.74	29.47
	Proportion (%)	0.10	0.09	0.05	0.04	0.01	0.28
Scrubland	Area (ha)	850.20	1049.11	1221.51	729.37	215.13	4065.32
	Proportion (%)	8.19	10.10	11.76	7.02	2.07	39.15
Bare Soil	Area (ha)	865.67	744.11	596.02	265.23	265.23	2736.24
	Proportion (%)	8.34	7.17	5.74	2.55	2.55	26.35
Burnt areas	Area (ha)	123.77	110.51	97.99	105.35	72.94	510.56
	Proportion (%)	1.19	1.06	0.94	1.01	0.70	4.92
TOTAL	Area (ha)	2543.96	2703.09	2669.20	1676.08	791.26	10383.58
	Proportion (%)	24.50	26.03	25.71	16.14	7.62	100.00

4.2.3. LULC distribution across aspect

Table 4-16: Spatial distribution of LULC classes' across the different aspects at the study area, their totals and percentage coverages

LULC TYPES		ASPECT (facing-direction)									TOTAL	
		Flat	North	North East	East	South East	South	South west	West	North West	Area (ha)	Proportion (%)
Water Bodies	Area (ha)	6,29	0,70	4,19	9,79	10,49	26,56	18,87	3,50	6,99	80,39	0,84
Cultivated Land	Area (ha)	36,35	102,06	100,66	219,50	339,04	594,19	445,99	374,69	271,93	2212,47	23,93
shadows	Area (ha)	0,00	0,00	0,70	0,00	0,70	26,56	18,87	3,50	0,70	50,33	0,49
Rock outcrops	Area (ha)	53,83	29,36	51,03	27,26	13,98	8,39	10,49	13,98	37,05	208,31	2,36
Built-up areas	Area (ha)	2,10	0,70	1,40	0,00	0,70	0,70	1,40	1,40	2,80	8,39	0,11
Green vegetation	Area (ha)	4,89	4,89	2,80	3,50	2,80	5,59	2,80	2,80	2,80	30,06	0,32
Scrubland	Area (ha)	205,52	225,79	246,06	487,93	472,55	564,83	580,90	649,41	649,41	3433,00	39,32
Bare Soil	Area (ha)	596,98	311,07	373,29	296,39	136,31	133,52	153,79	262,14	634,73	2263,50	27,91
Burnt areas	Area (ha)	15,38	6,29	14,68	16,78	34,95	174,06	134,22	64,31	30,06	460,67	4,73
Total	Area (ha)	921,34	680,87	794,81	1061,15	1011,51	1534,40	1367,33	1375,72	1636,46	8747,12	100,00
	Proportion (%)	8,87	6,56	7,65	10,22	9,74	14,78	13,17	13,25	15,76	100,00	

Table 4-16 presents the distribution of LULC types across aspect. The north-west facing slopes were characterised with the highest occurrence of LULC types with a proportion of about 17.8% followed by the south facing slopes at ~14.9%. In the southern hemisphere, south facing slopes have little sunlight and tend to be cooler than those facing north, where they are predominately exposed to direct sunlight. Most green vegetation, scrubland, cultivated areas and built-up areas which would be expected to be occurring mostly on the north facing slopes occur most on the south facing slope. This is contrary to the popular logic that follows distribution as per the relative position to direct sunlight.

The areas covered by bare soil, water bodies and built-up areas peak in both the northwest and north aspects, whereas the other LULC types peak most at the south and southwest aspects including the cultivated and all the vegetation classes. The peaking of the built-up areas on the north-facing slopes is understandable as human being tend to settle in slopes that expose them to direct sunlight for warm temperatures. However the cultivated land and vegetation classes are mostly situated on the slopes that are not directly exposed to the sunlight.

5. DISCUSSION

High resolution satellite images are increasingly becoming more available, thus making them an important resource to land management practitioners, analysts, researchers, planners and other professionals. It had been established that the conventional means of image interpretations are time- and labour- intensive, expensive, and subjective, making it difficult to fully exploit this valuable data, particularly over large geographic areas. Whilst the PBIA classification methods may offer satisfactory results for LULC mapping over large geographic areas, there had been some identified shortfalls in their ability in detailed mapping with high-resolution imagery. This saw the emergence of the OBIA classification techniques for use on high resolution images.

This study sought to compare and evaluate the performances of the PBIA and OBIA approaches in terms of mapping a mountainous landscape using the medium to high-resolution images: SPOT-6 and WorldView-2. In addition to the comparison of the two image analysis approaches, this study also compared the performances of two image datasets as to establish if it would be necessary to procure the WorldView-2 imagery or use the freely available SPOT-6 for similar studies in the future. In this study, the best of the four classification results was subjected to three separate overlay analyses in order to establish the relationship between the LULC and the three topographic variables of elevation, slope and aspect in the Mokhotlong District.

5.1. Comparison of the classification performances

Generally, all four classification outcomes yielded were able to generate, to some degree, relatively similar visual depictions of the broad LULC types that characterised the study area at the time when the images were captured. The LULC map achieved from the pixel-based SVM classification of SPOT-6 looked rather different from the other maps, the PBIA-WorldView-2 LULC map seemed as a balance between the OBIA LULC maps and the PBIA-SPOT-6. The LULC maps achieved from the object-based SVM classification presented very similar depictions of the broad LULC types in the study area. The LULC maps achieved from the pixel-based SVM classification were characterised with the salt-and-pepper effects, whereas the object-based counterparts were generally characterised with smoother appearances with well-defined boundaries between features.

The overall accuracy of the four classification models ranged between 79.5% for the pixel based SVM on SPOT-6 to 93.2% on the object based SVM on WorldView-2, with a

kappa coefficient that ranged from 0.776 to 0.925. With an exception of the pixel based SVM classification on the SPOT-6 multispectral image, all other models achieved an overall accuracy greater than 80%. The OBIA models reached the overall accuracies of reached an 89.7% and 93.2%, and kappa coefficients of 0.888 and 0.925 for SPOT-6 and WorldView-2, respectively. The pixel-based SVM classification of the WorldView-2 achieved the second lowest classification accuracy and kappa coefficient of 82.9% and 0.813, respectively.

Even though there is no recognized standard for accuracy assessment, a commonly suggested accuracy is 85% (Foody, 2002). According to the guidelines regarding accuracy, only the OBIA SVM classifications surpassed the suggested accuracy scores with the PBIA classifications falling short. In addition, the OBIA models significantly reduced the salt-and-pepper effects compared to the PBIA models. In this study, the OBIA approach was superior to the PBIA approach in terms of the extraction and mapping the LULC types on the mountainous study area, as it achieved better classification accuracy. These results are consistent with those achieved from other comparative studies of the two image analysis approaches on the other types of landscapes (e.g. Castillejo–Gonzalez *et al.,* 2009; Chen *et al.,* 2009; Robertson and King, 2011; Duro *et al.,* 2012, Adejopu *et al.,* 2015).

When comparing the classification performances of the SPOT-6 and WorldView-2 for LULC types on a mountainous landscape using the SVM classifiers, the PBIA classifications, the SPOT-6 achieved the overall accuracy of 79.5% and the WorldView-2 achieved 82.9%. For the OBIA classifications the accuracies were 89.7% and 93.2%, respectively. The above classification accuracies revealed that the WorldView-2 had better performance compared to the SPOT-6 when the SVM classifiers were applied using both classification accuracies. The better performance of Worldview-2 compared to SPOT-6 is consistent with the findings of other comparative studies of the performances of images of different resolutions. The findings of the comparative studies were that the improved spatial and spectral resolutions tend to improve the classification performances. WorldView-2 has an advantage over the SPOT-6 in both its spatial and spectral resolutions (see Table 3-1) thus giving better performances. A number of studies are consistent with the present on include: (Lu *et al.,* 2005; Ambunakudige *et al.,* 2009; Novack *et al.,* 2011; Gao and Mas, 2013; Capolsini *et al.,* 2014).

The evaluation of the performance using the McNemar's test revealed that the difference between SPOT-6 and WorldView-2 when both the PBIA and OBIA approaches are used was statistically significant at 95% level. It was found that the comparison of the

difference in the performances of the individual images using the different approaches was also statistical significant at 95% level.

5.2. The relationship between LULC distribution and topography

The analyses of the distribution of LULC types in relation to topography (i.e. elevation, slope and aspect) is essential for the understanding the interaction of humans and their surrounding environment. Mountainous regions are characterised with high heterogeneity in terms of elevation, slope and aspect which in turn then influence variations in microclimate, flora and varying soil properties which then lead to a wide variety of landforms over short distances.

The analysis of the relationship between the LULC types with respect to elevation revealed that that to some degree are topographically-controlled patterns of green vegetation, scrubland and built-up areas. Overlay analysis shows that topography (i.e. aspect, elevation and slope) influenced the spatial distribution of these classes those three LULC classes generally reduced in % area with increasing altitude and increasing steepness. Temperature may be a limiting factor. The rest of the LULC types used for the purpose of this study did not exhibit such strong evidence of the influence of elevation and this may be attributed to the fact that the landscape had been significantly altered by agricultural activities and fires.

Generally, the occurrence of most LULC types such as water bodies, rock outcrops and cultivated areas exhibited trends that maybe directly linked with the degrees of slope steepness. The bare soil and burnt areas decreased with the increasing steepness of the slopes. In terms of the distribution of LULC types with respect to aspect, no significant trends. Mostly, the relationship between the distributions of LULC types with topography is to some degrees convoluted. Practices such as agriculture and fires contributed significantly in terms of disrupting the topographically-controlled patterns of LULC types. The prominence of cultivated and burnt areas may have obscured the exposure of defined trends of the relationship between the distribution LULC types and topography. An additional reason may be that the relationships were studied using a resampled LULC map which meant that there may information lost during resampling. The overlay analyses were conducted on a 30 m spatial resolution which left opportunities for LULC features covering an area smaller than that to be overlooked during the analyses.

6. CONCLUSIONS AND RECOMMENDATIONS

6.1. Conclusions

This study sought to compare performances of the PBIA and OBIA approaches for the classification of a mountainous landscape of the Mokhotlong District of Lesotho using the high resolution images. The study also evaluated the significance of the difference in classification performances on the WorldView-2 and SPOT-6 imagery. In addition to the above comparisons, the study used the best LULC map in terms of accuracy and the topographic variables (elevation, slope and aspect) derived from a SRTM DEM in order to facilitate understanding of the relationship between the spatial distribution of the LULC types and topography.

The key findings of this study of this study were that:

- WorldView-2 had better overall performances compared to SPOT-6 high resolution images in terms of LULC classifications using both the PBIA and OBIA approaches. The differences in the performances of the two imagery packages were statistical significant 95% confidence level. This means that the difference in the spatial and spectral resolutions of the WorldView-2 and SPOT-6 has a significant difference in their performances in terms of mapping LULC in a mountainous landscape.
- The OBIA approach for LULC classification of high resolution satellite data was shown to be the more effective tool for analysing LULC in mountainous landscapes compared to the PBIA approach. The OBIA SVM classifier performed better than its PBIA counterpart on both WorldView-2 and SPOT-6, and difference in the performances to be statistically significant at the 95% significance level.
- The relationship between the distribution of LULC types and topography was found to have been seriously disturbed, particularly that of LULC types distribution and aspect. This is due to the fact that the landscape had been significantly altered by the occurrence of fire and deforestation for agricultural and settlement purposes.

6.2. Recommendations

- Collection of ground truth data is recommended in order to validate the accuracy of the classification results and to increase the confidence of the results. This would also help to determine whether the resolution of WorldView2 pan-sharpened imagery is appropriate for mapping for the collection of validation data or whether higher resolution imagery is needed in cases the field data are not available.

- A multi-temporal mapping of LULC in multiple seasons is recommended so that the areas that had lost their usual land covers to fires may be captured into these maps. Even if a multi-temporal study, it would desirable to conduct a LULC mapping study using imagery that had been captured in different season or when there had not been any fires.
- LULC mapping using imagery captured during times that had none or very limited fire outbreaks, deforestation and limited soil tilling for agricultural purposes may also be beneficial in terms of understanding of the relationships between the distribution of LULC types and topographical variables.
- The attainment of a finer scale DEM would also be very useful in terms of increasing the confidence on the results achieved from an overlay analysis of the relationship between LULC distribution and topography.

7. REFERENCES

Adam, E., Mutanga, O., Odindi, J. and Abdel-Rahman, E. M. (2014), Land-use/cover classification in a heterogeneous coastal landscape using RapidEye imagery: evaluating the performance of random forest and support vector machines classifiers. *International Journal of Remote Sensing*, 35(10), 3440–3458.

Adepoju, M. O., Sadiya, T. B., Mohammed, S. O., Halilu, S. A., Ibrahim, I. and Shar, J. T. (2015), Comparison and analysis of the pixel-based and object-oriented methods for land cover classification with ETM+ data. *IOSR Journal of Environmental Science, Toxicology and Food Technology*, 9(2), 48-53.

Aguirre-Gutiérrez, J., Seijmonsbergen, A. C. and Duivenvoorden, J. F. (2012), Optimizing land cover classification accuracy for change detection, a combined pixel-based and object based approach in a mountainous area in Mexico. *Applied Geography*, 34, 29-37.

Ambinakudige, S., Choi, J. and Khanal, S., (2009), *A comparative analysis of CBERS and Landsat data*. Baltimore, Maryland, ASPRS Annual Conference.

Belgiu, M. and Dragut, L. (2014), Comparing supervised and unsupervised multiresolution segmentation approaches for extracting buildings from very high resolution imagery. *ISPRS Journal of Photogrammetry and Remote Sensing*, 96, 67–75.

Bennie, J., Hill, H. O., Baxter, R. and Huntley, B. (2006), Influence of slope and aspect on long-term vegetation change in British chalk grasslands. *Journal of Ecology*, 94, 355-368.

Bennie, J., Huntleya, B., Wiltshirea, A. and Hill, M. (2008), Slope, aspect and climate: Spatially explicit and implicit models of topographic microclimate in chalk grassland. *Ecological Modelling*, 216, 47-59.

Benz, U. C., Hofmann, P., Willhauck, G., Lingenfelder, I. and Heynen, M. (2004), Multi-resolution, object-oriented fuzzy analysis of remote sensing data for GIS-ready information. *ISPRS Journal of Photogrammetry and Remote Sensing*, 58, 239-258.

Bhaskaran, S., Paramananda, S. and Ramnarayan, M. (2010), Per-pixel and objectoriented classification methods for mapping urban features using IKONOS satellite data. *Applied Geography*, 30(4), 650–665.

Blaschke, T. (2010), Object based image analysis for remote sensing. *ISPRS Journal of ISPRS Journal of Photogrammetry and Remote Sensing*, 65(1), 2-16.

Blaschke, T., Burnett, C. and Pekkarinen, A., (2006), Image segmentation methods for object based analysis and classification. In: S. M. Jong and F. D. Meer, eds. *Remote Sensing Image Analysis: Including the spatial domain.* Netherlands: Springer, 211-236.

Brenning, A., (2009). Benchmarking classifiers to optimally integrate terrain analysis and multispectral remote sensing in automatic rock glacier detection. *Remote Sensing of Environment,* 113(1), 239–247.

Cairong, Y. and Rong, Z., (2011). A study on object-oriented classification of land use/land cover of remote sensing image. *Southwest Forestry University,* 1(1), 1-4.

Capolsini, P., Andréfouët, S., Rion, C. and Payri, C., (2014). A comparison of Landsat ETM+, SPOT HRV, Ikonos, ASTER, and airborne MASTER data for coral reef habitat mapping in South Pacific islands. *Canadian Journal of Remote Sensing,* 29(2), 187-200.

Carreiras, J. M., Pereira, J. M., Campagnolo, M. L. and Shimabukuro, Y. E., (2006). Assessing the extent of agriculture/pasture and secondary succession forest in the Brazilian Legal Amazon using SPOT VEGETATION data. *Remote Sensing of Environment,* 101(3), 283–298.

Castillejo-González, I. L., López-Granados, F., García-Ferrer, A., Peña-Barragán, J. M., Jurado-Expósito, M. and de la Orden., (2009). Object- and pixel-based analysis for mapping crops and their agro-environmental associated measures using Quickbird imagery. *Computers and Electronics in Agriculture,* 68(2), 207–215.

Chena, M., Sua, W., Lia, L; Zhang, C., Yuea, A., Yuea, A. (2009). Comparison of pixel based and object-oriented knowledge-based classification methods using SPOT5 imagery. *WSEAS Transactions on Information Science and Applications,* 3(6), 477-489.

Cleve, C., Maggi, K., Kearns, F. R. and Moritz, M., 2008. Classification of the wildland–urban interface: A comparison of pixel- and object-based classifications using high-resolution aerial photography. *Computers, Environment and Urban Systems,* 32, 317-326.

Coblentz, D. and Keating, P. L., (2008). Topographic controls on the distribution of tree islands in the high Andes of South-Western Ecuador. *Journal of Biogeography,* 35, 2026-2038.

Coblentz, D. and Riitters, K. H., (2004). Topographic controls on the regional-scale biodiversity of the south-western USA. *Journal of Biogeography,* 31, 11251138.

de Leeuw, J., Jia, H., Schmidt, K., Skidmore, A.K, and Liu, X., (2006). Comparing accuracy assesments to infer superiority of image classification methods. *International Journal of Remote Sensing,* 27(1), 223-232.

Duro, D. C., Franklin, S. E. and Dubé, M. G., (2012). A comparison of pixel-based and object-based image analysis with selected machine learning algorithms for the classification of agricultural landscapes using SPOT-5 HRG imagery. *Remote Sensing of Environment,* 118, 259–272.

Foody, G. M., (2002). Status of land cover classification accuracy assessment. *Remote Sensing of Environment,* 80, 185-201.

Forsyth, A. T., Gibson, L. A. and Turner, A. A., (2014). Assessment of SPOT 6 imagery for mapping the invasive alien plant species Pinus spp. in a mountainous area of the Western Cape. *AfriGEO,* 1(1), 1-12.

Franklin, J., McCullough, P. and Gray, C., (2000) Terrain variables used for predictive mapping of vegetation communities in Southern California. In: J. P. Wilson and J. C. Gallant, eds. *Terrain analysis— principles and applications.* New York: Wiley, 331–353.

Gao, Y. and Mas, J. F., (2013). A comparison of the performance of pixel-based and object-based classifications over images with various spatial resolutions. *ISPRS,* 1-6.

Gislason, P. O., Benediktsson, J. A. and Sveinsson, J. R., (2007). Random Forests for land cover classification. *Pattern Recognition Letters,* 27, 294–300.

Guisan, A. and Zimmerman, N. E., (2000). Predictive habitat distribution models in ecology. *Ecological Modelling,* 135, 147.

Hasmadi, I. M., Pakhriazad, H. Z. and Shahrin, M. F., (2009). Evaluating supervised and unsupervised techniques for land cover mapping using remote sensing data. *Malaysian Journal of Society and Space,* 5(1), 1-10.

Hoersch, B., Braun, G. and Schmidt, U., (2002). Relation between landform and vegetation in alpine regions of Wallis, Switzerland. A multiscale remote sensing and GIS approach. *Computers, Environment and Urban Systems,* 26, 113-139.

Hsu, C., Chang, C. and Lin, C., (2010). A Practical Guide to Support Vector Classification. *National Taiwan University,* 1 (1), 1-16.

Huang, C., Davis, L. S. and Townshend, J. R., (2002). An assessment of support vector machines for land cover classification. *International Journal of Remote Sensing,* 23(4), 725-749.

Iqbal, M. F. and Khan, I. A., (2014). Spatiotemporal Land Use Land Cover change analysis and erosion risk mapping of Azad Jammu and Kashmir, Pakistan. *The Egyptian Journal of Remote Sensing and Space Sciences,* 17, 209–229.

Ivits, E. and Koch, B., (2002). *Object-oriented remote sensing tools for biodiversity assessment.* Prague, Czech Republic, Rotterdam, Netherlands: Millpress Science Publishers.

Karatzoglou, A., Smola, A., Hornik, K. and Zeileis, A., (2004). kernlab - An S4 Package for Kernel Methods in R. *Journal of Statistical Software*, 11(9), 1-20. Kobisi, K., (2005). *Preliminary checklist of the plants of Lesotho,* Pretoria and Roma: SABONET.

Laliberte, A. S., Fredrickson, E. L. and Rango, A., (2007). Combining decision trees with hierarchical object-oriented image analysis for mapping arid rangelands. *Photogrammetric Engineering and Remote Sensing,* 73(2), 197–207.

Lang, S., (2008). Object-based image analysis applications: modelling complexities. In: T. Blaschke, S. Lang and J. G. Hay, eds. *Object-Based Image Analysis.* Salzburg, Austria: Springer Berlin Heidelberg, 3-27.

Li, X. and Shao, G., (2014). Object-based land-cover mapping with high resolution aerial photography at a country scale in Midwestern USA. *Remote Sensing,* 6, 11372-11390.

Lowe, S., Guo, X. and Henderson, D., (2012). Landscape spatial structure for predicting suitable habitat: The case of Dalea Villosa in Saskatchewan. *Open Journal of Ecology,* 2(2), 60-73.

Lu, D., Batistella, M. and de Moran, E. E., (2005). A comparative study of Terra ASTER, Landsat TM, and SPOT HRG data for land cover classification in the Brazilian Amazon. *The 9th World Multi-Conference on Systematics and Informatics,* 411-416.

Maestre, F. T., Cortina, J., Bautista, S., Bellot, J. and Vallejo, R., (2003). Small-scale environmental heterogeneity and spatiotemporal dynamics of seedling establishment in a semiarid degraded ecosystem. *Ecosystems,* 6, 630-643.

Mararakanye, N. and Le Roux, J. J., (2011). *Manual digitising of gully erosion in South Africa using high resolution SPOT 5 satellite imagery at 1: 10 000 scale,* Pretoria: South Africa's Department of Agriculture, Forestry and Fisheries.

Mararakanye, N. and Nethengwe, N. S., (2012). Gully features extraction using remote sensing techniques. *South African Journal of Geomatics,* 1(2), 109118.

Matinfar, H. R., Sarmadian, F., Alavi-Panah, S. K. and Heck, R. J., (2007). Comparison of object-oriented and pixel-based classification of land use/land cover types based on Lansadsat7, ETM+ spectral bands (Case Study: Arid Region of Iran).. *American-Eurasian Journal Agricultural and Environmental sciences,* 2(4), 448-456.

Matsuura, T. and Suzuki, W., (2013). Analysis of topography and vegetation distribution using a digital elevation model: case study of a snowy mountain basin in northeastern Japan. *Landscape Ecology Engineering,* 9, 143–155.

McCune, B. and Kean, D., (2002). Equations for potential annual direct incident radiation and heat load. *Journal of Vegetation Science,* 13, 603-606.

Moeletsi, M. E. and Walker, S., (2013). Agroclimatological suitability mapping for dryland maize production in Lesotho. *Theoretical and Applied Climatology,* 114, 227-236.

Mutanga, O., Aam, E. and Cho, M. A., (2012). High density biomass estimation for wetland vegetation using WorldView-2 imagery and random forest regression algorithm. *International Journal of Applied Earth Observation and Geoinformation,* 18, 399-406.

Myburgh, G. and Van Niekerk, A., (2013). Effect of feature dimensionality on objectbased land cover classification: a comparison of three classifiers. *South African Journal of Geomatics,* 2(1), 13-27.

Myint, S. W., Gorber, P., Brazel, A., Grossman-Clarke, S. and Weng, Q., (2011). Per-pixel vs. object-based classification of urban land cover extraction using high spatial resolution imagery. *Remote Sensing of Environment,* 115, 1145–1161.

Nagakura, M., (2010). The natural environment and the livelihoods of people living in a mountainous region of Lesotho. *African Study Monographs,* 40, 179-194.

Nanyam, Y., Pandiripalli, S., Telagarapu, P. and Kota, S., (2011). Land use and land cover classification using remotely sensed image. *MIPSCCON,* 1(1), 14-17.

Novack, T., Esch, T., Kux, H. and Stilla, U., (2011). Machine learning comparison between WorldView-2 and QuickBird-2-Simulated imagery regarding objectbased urban land cover classification. *Remote Sensing,* 3, 2263-2282.

Otukei, J. R. and Blascke, T., (2010). Land cover change assessment using decision trees, support vector machines and maximum likelihood classification algorithms. *International Journal of Applied Earth Observation and Geoinformation,* 12s, s27-s31.

Pal, M., (2006). Support vector machine-based feature selection for land cover classification: a case study with DAIS hyperspectral data. *International Journal of Remote Sensing,* 27, 2877-2894.

Pérez, A., Mas, J. F., Velazquez, A. and Vazquez, L., (2008). Modeling vegetation diversity types in Mexico based upon topographic features. *Inverciencia,* 33(2), 88-95.

Petropoulos, G. P., Arvanitis, K. and Sigrimis, N., (2012a). Hyperion hyperspectral imagery analysis combined with machine learning classifiers for land use/cover mapping. *Expert Systems with Applications,* 39, 3800-3809.

Petropoulos, G. P., Kalaitzidis, C. and Vadrevu, P. K., (2012b). Support vector machines and object-based classification for obtaining land-use/cover cartography from Hyperion hyperspectral imagery. *Computers and amp; Geosciences,* 41, 99-107.

Pignatti, S., Cavalli, R M; Cuomo, V; Fusilli, L; Pascucci, S; Poscolieri, M; Santini, F., (2009). Evaluating Hyperion capability for land cover mapping in a fragmented ecosystem: Pollino National Park, Italy. *Remote Sensing of Environment,* 113, 622-634.

Platt, R. V. and Rapoza, L., (2008). An evaluation of an object-oriented paradigm for land use/land cover classification. *The Professional Geographer,* 60(1), 87.

Pradhan, B. and Suleiman, Z., (2009). Land cover mapping and spectral analysis using multi-sensor. *Journal of Geomatics,* 3(2), 71-78.

Pradhan, T., Walia, V., Kapoor, R. and Saran, S., (2014). Optimizing land use classification using decision tree approaches. *IEEE,* 1(1), 1-15.

Prakasam, C., (2010), Land use and land cover change detection through remote sensing approach: A case study of Kodaikanal Taluk, Tamil Nadu. *International Journal of Geomatics and Geosciences,* 1, 150-158.

Rahman, R. and Saha, S. K., (2008). Multi-resolution segmentation for object-based classification and accuracy assessment of land use/land cover classification using remotely sensed data. *Journal Indian Society of Remote Sensing,* 36, 189-201.

Ramaswamy, S. K. and Ranganathan, M. B., (2014). Land use land cover classification using local multiple patterns from very high resolution satellite imagery. *The International Archives of the Photogrammetry, Remote Sensing and Spatial Information Sciences,* XL (8), 971-976.

Robertson, L. D. and King, D. J., (2011). Comparison of pixel- and object-based classification in land cover change mapping. *International Journal of Remote Sensing,* 32(6), 1505–1529.

Rozenstein, O. and Karnieli, A., (2011). Comparison of methods for land-use classification incorporating remote sensing and GIS inputs. *Applied Geography,* 31, 533-544.

Salehi, B., Zhang, Y., Zhong, M. and Dey, V., (2012). Object-based classification of urban areas using VHR imagery and height points ancillary data. *Remote Sensing*, 4, 2256-2276.

Salman, A., Crossing, K. and Nadeem, Q., (2002). *Integration of DEMs, satellite imagery and field data for Alpine vegetation mapping.* San Diego, Carlifonia, ESRI press. 1-10.

Şatır, O. and Berberoğlu, S., (2012). Land use/cover classification techniques using optical remotely sensed data in landscape planning. In: M. Ozyavuz, ed. *Landscape Planning.* Rijeka, Croatia: InTech, 21-54.

Schowengerdt, A., (2007). *Remote sensing, models, and methods for image processing.* 3rd ed. San Diego, California: Elsevier, Academic Press.

Sene, K. J., Jones, D. A., Meigh, J. R. and Farquharso, F. A., (1998). Rainfall and flow variations in the Lesotho highlands. *International Journal of Climatology,* 18, 329-345.

Shresta, D. P. and Zinck, J. A., (2001). Land use classification in mountainous areas: integration of image processing, digital elevation data and field knowledge (application to Nepal). *Journal of Applied Geography,* 3(1), 78-85.

Sohl, T. L. Sleeter, B. M., Zhu, Z., Sayler, K. L., Bennett, K. L., Bouchard, M., Hawbaker, T., Wein, A., Liu, S., Kanengieter, R. and Acevedo, W., (2010). A land-use and land-cover modelling strategy to support a national assessment of carbon stocks and fluxes. *Applied Geography,* 34, 111- 124.

Tehrany, M. S., Pradhan, B. and Jebuv, M. N., (2014). A comparative assessment between object and pixel-based classification approaches for land use/land cover mapping using SPOT 5 imagery. *Geocarto International,* 29(4), 351369.

Tovar, C., Seijmonsbergen, A. C. and Duivenvoorden, J. F., (2013). Monitoring land use and land cover change in mountain regions: An example in the Jalca grasslands of the Peruvian Andes. *Landscape and Urban Planning,* 112, 40–49.

Trimble, (2014). *eCognition Developer 9.0 Reference Book,* Munich, Germany: Trimble Germany GmbH.

Tzotsos, A., (2006). *A support vector machine approach for object based image analysis,* s.l.: Commission IV, WG IV/4 – Commission VIII, WG VIII/1.

Van Zwieten, (2014). Unlocking the promise that space holds for sustainable development. [Online] Available at: http://www.ee.co.za/article/unlocking-promise-space-holds-sustainabledevelopment-economic-growth.html [Accessed 14 April 2015].

Volker, W., (2003). Object-based classification of remote sensing data for change detection. *ISPR Journal of Photogrammetry and Remote Sensing,* 58, 225238.

Wondie, M., Teketay, D., Melesse, A. M. and Schneider, W., (2012). Relationship between topographic variables and land cover in the Simen Mountains National Park, a World Heritage Site in Northern Ethiopia. *International Journal of Remote Sensing Applications,* 2, 36-43.

Xie, Y., Sha, Z. and Yu, M., (2008). Remote sensing imagery in vegetation mapping: a review. *Journal of Plant Ecology,* 1(1), 9–23.

Yadav, P. K., Kapoor, M. and Sarma, K., (2010). Land use land cover mapping, change detection and conflict analysis of Nagzira-Navegaon Corridor, Central India using geospatial technology. *International Journal of Remote Sensing and GIS,* 1(2), 90-98.

Yan, G. Mas , J. F., Maathuis, B. H., Xiangmin, Z., and Van Dijk, P. M., (2007). Comparison of pixel-based and object-oriented image classification approaches-A case study in a Coal Fire Area, Wuda, Inner Mongolia, China. *International Journal of Remote Sensing*, 27, 4039–4055.

Zhao, N., Yang, Y. and Zhou, X., (2010). Application of geographically weighted regression in estimating the effect of climate and site conditions on vegetation distribution in Haihe catchment, China. *Plant Ecology*, 209, 349-359.